Title

Loss-of-function in RBBP5 results in a syndromic neurodevelopmental disorder associated with microcephaly.

Journal

Genetics in Medicine, 26(11)

Authors

Huang, Yue
Jay, Kristy
Yen-Wen Huang, Alden
et al.

Publication Date

2024-11-01

DOI

10.1016/j.gim.2024.101218

Peer reviewed

HHS Public Access

Author manuscript

Genet Med. Author manuscript; available in PMC 2024 December 16.

Published in final edited form as:

Genet Med. 2024 November ; 26(11): 101218. doi:10.1016/j.gim.2024.101218.

*Correspondence and requests for materials should be addressed to Julian A Martinez-Agosto, Division of Clinical Genetics, Department of Human Genetics, Department of Psychiatry, Semel Institute for Neuroscience and Human Behavior, David Geffen School of Medicine at UCLA, Gonda Neuroscience and Genetics Research Center, Room 4554, 695 Charles E. Young Drive South, Los Angeles, CA 90095. julianmartinez@mednet.ucla.edu OR Michael Wangler, Department of Molecular and Human Genetics, Baylor College of Medicine, Jan and Dan Duncan Neurological Research Institute, Texas Children's Hospital, Room: DNRI-1050, 1250 Moursund St #1125, Houston, TX 77030. michael.wangler@bcm.edu.

Yue Huang and Kristy L. Jay contributed equally to this article.

Author Contributions

Conceptualization: Y.H., K.L.J., M.F.W., J.A.M.-A.; Data Curation: Y.H., J.A.M.-A.; Formal Analysis: Y.H., K.L.J., M.F.W., J.A.M.-A.; Funding Acquisition: J.A.M.-A., S.F.N., C.G.P., M.F.W., S.Y., H.J.B., Y.H.; Investigation: Y.H., K.L.J., A.Y.-W.H., J.W., S.V.J., O.C., A.R., O.B., M.M., M.I., H.X., J.H., C.M., K.B., V.S., A.Y.M.-S., F.R., S.S., C.C., J.A.R; Resources: Y.H., K.L.J., O.K., H.J.B., M.F.W. J.A.M.-A.; Supervision: S.Y., H.J.B., C.G.P., S.F.N. M.F.W., J.A.M.-A.; Writing-original draft: Y.H., K.L.J.; Writing-review and editing: Y.H., K.L.J., A.Y.-W.H., J.W., S.V.J., O.C., A.R., O.B., M.M., M.I., H.X., J.H., C.M., K.B., V.S., A.Y.M.-S., F.R., S.S., C.C., S.Y., O.K., H.J.B., J.A.R., C.G.S., S.F.N., M.F.W., J.A.M.-A.

Ethics Declaration

Probands were recruited through their local referring physicians and the Undiagnosed Diseases Network (UDN) clinical site (UCLA). Individual 1 (UDN903866) was identified through the UDN, and individuals 2 through 5 were identified through GeneMatcher. Before inclusion, informed written consent was obtained from the legal guardians of the individuals included in this study for research and publication according to the standards and practices of the institutional review board and ethics committee at UCLA. Documents and consent forms were standardized according to the requirements of the UDN. Consents for publishing photograph were obtained from all patients and/or their legal guardians.

Conflict of Interest

The Department of Molecular and Human Genetics at Baylor College of Medicine receives revenue from clinical genetic testing conducted at Baylor Genetics Laboratories.

Consortium Member Listing

The Undiagnosed Diseases Network authors include: Maria T. Acosta, David R. Adams, Raquel, L. Alvarez, Justin Alvey, Aimee Allworth, Ashley Andrews, Euan A. Ashley, Carlos A. Bacino, Guney Bademci, Ashok Bala-subramanyam, Dustin Baldridge, Jim Bale, Michael Bamshad, Deborah Barbouth, Pinar Bayrak-Toydemir, Anita Beck, Alan H. Beggs, Edward Behrens, Gill Bejerano, Hugo J. Bellen, Jimmy Bennett, Jonathan A. Bernstein, Gerard T. Berry, Anna Bican, Stephanie Bivona, Elizabeth Blue, John Bohnsack, Devon Bonner, Lorenzo Botto, Lauren C. Briere, Gabrielle Brown, Elizabeth A. Burke, Lindsay C. Burrage, Manish J. Butte, Peter Byers, William E. Byrd, John Carey, Olveen Carrasquillo, George D. Carvhalo Neto, Thomas Cassini, Ta Chen Peter Chang, Sirisak Chanprasert, Hsiao-Tuan Chao, Ivan Chinn, Gary D. Clark, Terra R. Coakley, Laurel A. Cobban, Joy D. Cogan, Matthew Coggins, F. Sessions Cole, Heather A. Colley, Heidi Cope, Rosario Corona, William J. Craigen, Andrew B. Crouse, Michael Cunningham, Precilla D'Souza, Hongzheng Dai, Surendra Dasari, Joie Davis, Jyoti G. Dayal

Esteban C. Dell'Angelica, Katrina Dipple, Daniel Doherty, Naghmeh Dorrani, Argenia L. Doss, Emilie D. Douine, Dawn Earl, David J. Eckstein, Lisa T. Emrick, Christine M. Eng, Marni Falk

Elizabeth L. Fieg, Paul G. Fisher, Brent L. Fogel, Irman Forghani, William A. Gahl, Ian Glass, Bernadette Gochuico, Page C. Goddard, Rena A. Godfrey, Alana Grajewski, Don Hadley, Meghan C. Halley, Rizwan Hamid, Kelly Hassey, Nichole Hayes, Frances High, Anne Hing, Fuki M. Hisama, Ingrid A. Holm, Jason Hom, Martha Horike-Pyne, Alden Huang, Sarah Hutchison, Wendy Introne, Rosario Isasi, Kosuke Izumi, Gail P. Jarvik, Jeffrey Jarvik, Suman Jayadev, Orpa Jean-Marie, Vaidehi Jobanputra, Emerald Kaitryn, Shamika Ketkar, Dana Kiley, Gonench Kilich, Shilpa N. Kobren, Isaac S. Kohane, Jennefer N. Kohler, Susan Korrick, Deborah Krakow, Donna M. Krasnewich, Elijah Kravets, Seema R. Lalani, Byron Lam, Christina Lam, Brendan C. Lanpher, Ian R. Lanza, Kimberly LeBlanc, Brendan H. Lee, Roy Levitt, Richard A. Lewis, Pengfei Liu, Xue Zhong Liu, Nicola Longo, Sandra K. Loo, Joseph Loscalzo, Richard L. Maas, Ellen F. Macnamara, Calum A. MacRae, Valerie V. Maduro, Audrey Stephannie Maghiro, Rachel Mahoney, May Christine V. Malicdan, Laura A. Mamounas, Teri A. Manolio, Rong Mao, Ronit Marom, Gabor Marth, Beth A. Martin, Martin G. Martin, Julian A. Martínez-Agosto, Shruti Marwaha, Jacob McCauley, Allyn McConkie-Rosell, Alexa T. McCray, Elisabeth McGee, Matthew Might, Danny Miller, Ghayda Mirzaa, Ryan M. Moore, Eva Morava, Paolo Moretti, John J. Mulvihill, Mariko Nakano-Okuno, Stanley F. Nelson, Shirley Nieves-Rodriguez, Donna Novacic, Devin Oglesbee, James P. Orengo, Laura Pace, Stephen Pak, J. Carl Pallais, Christina G.S. Palmer, Jeanette C. Papp, Neil H. Parker, John A. Phillips III, Jennifer E. Posey, Lorraine Potocki, Barbara N. Pusey Swerdzewski, Aaron Quinlan

Deepak A. Rao, Anna Raper, Wendy Raskind, Genecee Renteria, Chloe M. Reuter, Lynette Rives, Amy K. Robertson, Lance H. Rodan, Jill A. Rosenfeld, Elizabeth Rosenthal, Francis Rossignol, Maura Ruzhnikov, Ralph Sacco, Jacinda B. Sampson, Mario Saporta, Judy Schaechter, Timothy Schedl, Kelly Schoch, Daryl A. Scott, Elaine Seto, Vandana Shashi, Emily Shelkowitz, Sam Sheppeard, Jimann Shin, Edwin K. Silverman, Janet S. Sinsheimer, Kathy Sisco, Edward C. Smith, Kevin S. Smith, Lilianna Solnica-Krezel, Ben Solomon, Rebecca C. Spillmann, Andrew Stergachis, Joan M. Stoler, Kathleen Sullivan, Jennifer A. Sullivan, Shirley Sutton, David A. Sweetser, Virginia Sybert, Holly K. Tabor, Queenie K.-G. Tan, Amelia L. M. Tan, Arjun Tarakad, Mustafa Tekin, Fred Telischi, Willa Thorson, Cynthia J. Tifft, Camilo Toro, Alyssa A. Tran, Rachel A. Ungar, Tiina K. Urv, Adeline Vanderver, Matt Velinder, Dave Viskochil, Tiphanie P. Vogel, Colleen E. Wahl, Melissa Walker, Nicole M. Walley, Jennifer Wambach, Jijun Wan, Lee-kai Wang, Michael F. Wangler, Patricia A. Ward, Daniel Wegner, Monika Weisz Hubshman, Mark Wener, Tara Wenger, Monte

Loss-of-function in *RBBP5* results in a syndromic neurodevelopmental disorder associated with microcephaly

Yue Huang[1], **Kristy L. Jay**[2,3], **Alden Yen-Wen Huang**[1], **Jijun Wan**[1], **Sharayu V. Jangam**[2,3], **Odelia Chorin**[4], **Annick Rothschild**[4], **Ortal Barel**[5,6], **Milena Mariani**[7], **Maria Iascone**[8], **Han Xue**[9], **Undiagnosed Diseases Network**, **Jing Huang**[9], **Cyril Mignot**[10,11], **Boris Keren**[12], **Virginie Saillour**[13], **Annelise Y. Mah-Som**[14], **Stephanie Sacharow**[15], **Farrah Rajabi**[16], **Carrie Costin**[17], **Shinya Yamamoto**[2,3], **Oguz Kanca**[2,3], **Hugo J. Bellen**[2,3], **Jill A. Rosenfeld**[2,18], **Christina G.S. Palmer**[1,19], **Stanley F. Nelson**[1], **Michael F. Wangler**[2,3,*], **Julian A. Martinez-Agosto**[1,19,*]

[1]Department of Human Genetics, David Geffen School of Medicine at UCLA, Los Angeles, CA

[2]Department of Molecular and Human Genetics, Baylor College of Medicine, Houston, TX

[3]Jan and Dan Duncan Neurological Research Institute, Texas Children's Hospital, Houston TX

[4]Institute for Rare Diseases, Sheba Medical Center, Tel HaShomer, Ramat Gan, Israel

[5]Genomics Unit, The Center for Cancer Research, Sheba Medical Center, Tel HaShomer, Israel

[6]Sheba Medical Center, Wohl Institute of Translational Medicine, Ramat Gan, Israel

[7]Pediatric Department, ASST Lariana, Santa Anna General Hospital, Italy

[8]Laboratorio di Genetica Medica, ASST Papa Giovanni XXIII, Bergamo, Italy

[9]Shanghai Institute of Precision Medicine at Ninth People's Hospital, Shanghai Jiao Tong University School of Medicine, Shanghai, China

[10]AP-HP Sorbonne Université, Département de Génétique, France

[11]Centre de Référence Déficiences Intellectuelles de Causes Rares, France

[12]Genetic Department, GCS SeqOIA, Pitié-Salpêtrière Hospital, AP-HP, Sorbonne University, Paris, France

[13]Laboratoire de biologie médicale multisites Seqoia - FMG2025, Paris, France

[14]Harvard Medical School Genetics Training Program, Boston, MA

[15]Division of Genetics and Genomics, Boston Children's Hospital, Boston, MA

[16]Section of Clinical Genetics and Metabolism, Department of Pediatrics, Children's Hospital Colorado and University of Colorado School of Medicine, Aurora, CO

[17]Division of Medical Genetics, Akron Children's Hospital, Akron, OH

Westerfield, Matthew T. Wheeler, Jordan Whitlock, Lynne A. Wolfe, Kim Worley, Changrui Xiao, Shinya Yamamoto, John Yang, Zhe Zhang, and Stephan Zuchner.

Additional Information

The online version of this article (https://doi.org/10.1016/j.gim.2024.101218) contains supplemental material, which is available to authorized users.

[18]Baylor Genetics Laboratories, Houston, TX

[19]Department of Psychiatry and Biobehavioral Sciences, Semel Institute for Neuroscience and Human Behavior, David Geffen School of Medicine at UCLA, Los Angeles, CA

Abstract

Purpose: Epigenetic dysregulation has been associated with many inherited disorders. *RBBP5* (HGNC:9888) encodes a core member of the protein complex that methylates histone 3 lysine-4 and has not been implicated in human disease.

Methods: We identify 5 unrelated individuals with de novo heterozygous variants in *RBBP5*. Three nonsense/frameshift and 2 missense variants were identified in probands with neurodevelopmental symptoms, including global developmental delay, intellectual disability, microcephaly, and short stature. Here, we investigate the pathogenicity of the variants through protein structural analysis and transgenic *Drosophila* models.

Results: Both missense p.(T232I) and p.(E296D) variants affect evolutionarily conserved amino acids located at the interface between RBBP5 and the nucleosome. In *Drosophila,* overexpression analysis identifies partial loss-of-function mechanisms when the variants are expressed using the fly *Rbbp5* or human *RBBP5* cDNA. Loss of *Rbbp5* leads to a reduction in brain size. The human reference or variant transgenes fail to rescue this loss and expression of either missense variant in an *Rbbp5* null background results in a less severe microcephaly phenotype than the human reference, indicating both missense variants are partial loss-of-function alleles.

Conclusion: Haploinsufficiency of *RBBP5* observed through de novo null and hypomorphic loss-of-function variants is associated with a syndromic neurodevelopmental disorder.

Keywords

Epigenetic; H3K4 methylation; Microcephaly; Neurodevelopmental disorder; RBBP5

Introduction

The epigenetic machinery has an essential role in the spatiotemporal regulation of gene expression. One of the main epigenetic regulatory mechanisms is the post-translational modifications of histones, including methylation, acetylation, phosphorylation, and ubiquitylation.[1] These histone modifications allow precise and dynamic regulation of the accessibility of genomic regions to DNA-dependent processes, including transcription, replication, DNA repair, and recombination.[2] The methylation of histone 3 lysine-4 (H3K4) is an evolutionarily conserved chromatin mark that is typically found in active transcription sites and is considered a marker for gene activation.[3] H3K4 methylation is predominantly mediated by the complex of proteins associated with SET1 (COMPASS) protein complex, which includes one of the 6 SET1 domain-containing methyltransferases (KMT2A-F) and 3 other core members, WDR5, ASH2L, and RBBP5, to modulate the catalytic activity of methyltransferases.[4]

The number of Mendelian disorders caused by disruption of epigenetic machinery have greatly expanded in the past decade.[5] The functional classification divides the genes

into 4 groups: writer, eraser, reader, and remodeler.[5] Various histone methylation writers, including the SET1 domain-containing methyltransferases in COMPASS, have been associated with genetic disorders, such as Kabuki syndrome (OMIM#147920).[6] However, the nonmethyltransferase core members of COMPASS have not been linked to a human disorder to date. A heterozygous pathogenic variant in *KMT2D* (HGNC:7133) accounts for 50% to 70% cases with Kabuki syndrome, and 20% to 30% of patients with a clinical diagnosis of Kabuki syndrome have no identified known variant that causes the disease.[6] It has been hypothesized that a pathogenic mutation in other core members of the COMPASS protein complex could contribute to cases with Kabuki-like phenotypes.[7]

In this study, we report 5 unrelated patients with de novo heterozygous variants in *RBBP5*. These individuals present with neurodevelopmental features, including intellectual disability, developmental delay, microcephaly, and short stature. We provide evidence to support the pathogenicity of the variants through bioinformatic analysis, protein structure modeling, and functional studies in *Drosophila.* The difficulty in diagnosing individual 1 led to his enrollment in the Undiagnosed Diseases Network (UDN). The goal of the UDN is to facilitate collaboration between clinicians and researchers to improve diagnosis and care.[8–10] In addition to taking advantage of state-of-the-art phenotyping and genotyping tools, the UDN uses model organisms such as *Drosophila melanogaster* to perform functional assays on rare genetic variants identified in rare disease patients.[11,12] Fly researchers have generated an extensive transgenic toolkit for *Drosophila*, allowing for rapid functional characterization of candidate pathological variants.[13–16] Functional validation of genetic variants is a critical step toward confirming diagnosis and efforts to characterize novel disease genes improve diagnostic success of additional patients in the future.[12,17–20] Elucidating the mechanism for rare and undiagnosed diseases leads to improved diagnostic rates, earlier intervention, possible targeted therapeutics, and ultimately improved quality of life.[20]

Materials and Methods

Identification of individuals

Individual 1 was referred to the UDN at UCLA by a local physician. Other individuals were identified in Gene-Matcher,[21] and clinical information were collected through collaborators. In addition, a thorough search for candidate *RBBP5* variants was conducted in the clinical exome/genome database at the Baylor Genetics Laboratories. All individuals provided written consent for participation of research and publication, including consent to publish patient photos. This study has been approved by the institution review board at UCLA. *RBBP5* variants were identified by either exome or genome sequencing using genome build GRCh37/hg19. All individuals except 1 had both biological parents as comparators in the sequencing, and the variants were confirmed to be de novo because of absence in the parental sequences. Sanger sequencing was not performed because of high quality of variant calling.

Structural analysis

Structural analysis of human MLL3-ubNCP complex (PDB: 6KIW) was carried out with PyMOL (The PyMOL Molecular Graphics System, Version 2.0 Schrödinger, LLC, https://pymol.org/2/).

Drosophila melanogaster—Fly lines were obtained from the Bloomington Drosophila stock center and the Kyoto Drosophila stock center: daughterless-GAL4(3) (*daughterless*^{GAL4}) (Bellen lab), w[*]; P{w[mC]=UAS-mCherry.NLS}3 (BDSC: 38424) (*UAS-mCherry.NLS*), y[1]w[*]; P{w[+mC]=Act5C-GAL 4}25Fo1/Cyo, y[+] (BDSC:4414) (*Actin*^{GAL4}), y[1]w[1118]; P{w[+mC] ey3.5-GAL4.Exel}2 (BDSC: 8220) (*eyeless*^{GAL4}), P{w[+mC] GAL4-elav.L}2/Cyo (BDSC: 8765) (*elav*^{GAL4}), w[1118]; P{w[+m*] GAL4}repo/TM3, Sb (BDSC: 7415) (*repo*^{GAL4}), UAS-lacZ (Bellen lab) w[*];Cyo, P{w[+mC] Tb[1]Cpr[Cyo-A]/sna[Sco] (BDSC: 36335) (*Cyo, Tb*), w[1118]; Df(3L)BSC447/TM6C, Sb[1] cu[1] (BDSC:24951) (*Df (3L)BSC447*), y^{1} w*; PBac {y$^{+mDint2}$ w^{+mC} UAS-hsp-Hsap\RBBP5.HA.1}VK00037 / CyO, P{ry$^{+t7.2}$ sevRas1.V12}FK1 (DGRC: 305207) (*RBBP5-HA*). Stocks were held at 25°C, and all experiments were carried out at 25°C unless specified.

***Rbbp5*$^{Kozak\ GAL4}$ transgenic line generation—**The *Rbbp5*$^{Kozak\ GAL4}$ was generated as previously described.[22] Briefly, the *Rbbp5* coding sequence was replaced with a *Kozak sequence-GAL4-polyA-FRT-3XP3EGFP-polyA-FRT* (*KozakGAL4*) cassette using CRISPR-mediated homologous recombination. The homology donor intermediate construct is prepared by synthesis of sgRNA targeting the 5′ and 3′ untranslated regions (AAAATGAATTTGGAGCTACTAGG and TTATTTCTTGGTACGTCCGGCGG, respectively) and short (200 bp) homology arms in pUC57_Kan_gw_OK2 vector. The *KozakGAL4-polyA-FRT-3XP3EGFP-polyA-FRT* cassette is subcloned in the homology donor intermediate to generate the homology donor construct. Homology donor construct is injected (250 ng/μl) in embryos containing Cas9 in their germline (*y*^{1}*w**; *attP40(y+){nos-Cas9(v+)}; iso5)* and the resulting G0 progeny are crossed to *y*^{1}*w** flies and lines are screened for *3XP3-EGFP (enhanced green fluorescent protein)*-driven expression of EGFP. The correct integration of the *KozakGAL4* cassette in the proper locus is verified by polymerase chain reaction using forward and reverse primers flanking the homology arms and construct specific forward and reverse primers as described in Kanca et al.[22] The *RBBP5*$^{Kozak\ GAL4}$ transgenic line was submitted to the Bloomington Drosophila Stock Center (BDSC: 97331).

Human *RBBP5* and *Drosophila Rbbp5* construct generation

Human pcDNA3-FLAG-RBBP5 plasmid used in the protein expression experiments was obtained from Addgene (Cat# 15550). Candidate variants were introduced using Quik-Change II Site-directed mutagenesis kit according to manufacturer's protocol (Agilent). The mutations were confirmed by Sanger sequencing. For *Drosophila* experiments, Human cDNA for *RBBP5* (NM_005057.4) was obtained from the collection of the late Dr Kenneth Scott at Baylor College of Medicine (clone: IOH28957). Q5 site-directed mutagenesis was completed to create the variant sequence from the reference c.695C>T p.(T232I), c.888A>T p.(E296D). Constructs were transformed using high efficiency *E. coli* competent

cells (New England Biolabs, Cat # C2987H) from the pDONR 221 entry vector to the pGW-HA.attB destination vector using Gateway cloning and the sequences were confirmed by Sanger sequencing. Vectors were injected into embryos to create *P{UASt-RBBP5-Ref}VK37, P{UASt-RBBP5-T232I}VK37,* and *P{UASt-RBBP5-E296D}VK37*. For fly cDNA construct generation, *Rbbp5* (NM_140952.3) wild type and variant (p.T231I and p.E295D) lines were obtained (clone OFa19095D, GenScript USA, Inc). Constructs were transformed using high efficiency *E. coli* competent cells from the pGenDONR vector to the Gateway compatible pDONR 223 entry vector and subcloned to the pGW-HA.attB destination vector. Sequences were confirmed using Sanger sequencing, and vectors were injected into embryos to create *P{UASt-Rbbp5}VK37, P{UASt-Rbbp5-T231I} VK37,* and *P{UASt-RBBP5-E295D}VK37.* Transgenic males are crossed to y^1 *w** stocks, and construct integration is confirmed through selection for the mini white gene.

RBBP5 protein expression and western blot

Flag-tagged wild type and mutated human *RBBP5* plasmid were transfected to HEK293 cells by lipofectamine 3000 according to manufacturer's protocol (Invitrogen). Cells were lysed by RIPA buffer, and 20 mg of whole-cell lysate were used to assess protein expression in western blot. ANTI-FLAG M2 antibody from Sigma and anti-beta-actin from Santa Cruz Biotechnology were used to detect FLAG-tagged RBBP5 and Beta-actin, respectively. For *Drosophila* experiments, histone extraction was performed (Abcam, Cat# Ab113476) with 5 whole 3rd instar larvae ($n = 6$ replicates) using the manufacturer's protocol. Protein (10 μL) was loaded of each sample and RBBP5 (Cell Signaling Technology [CST], Cat#12766), H3K4me3 (CST, Cat# 9733), and histone H3 (CST, Cat# 9715) primary antibodies were used with goat anti-rabbit horse-radish peroxidase and imaged on a Bio-Rad Chemidoc MP imaging system. H3K4me3 normalization to total H3 was completed using ImageJ.

RBBP5/Rbbp5 overexpression viability and morphology evaluation in *Drosophila*

Heterozygous or homozygous (in the case of larval and pupal lethal crosses) male UAS-cDNA stocks were crossed to female GAL4 ubiquitous ($Actin^{GAL4}$ and $daughterless^{GAL4}$) and tissue-specific ($eyeless^{GAL4}$, $elav^{GAL4}$, and $repo^{GAL4}$) lines. The resulting progeny were counted by genotype ($n > 50$). Viability was calculated by comparing the observed number progeny with the expected (o/e ratio) based on Mendelian inheritance patterns. A normalized o/e ratio greater than 0.8 is defined as viable, semi-lethality is 0.8 to 0.15, and lethality is less than 0.15, and the latest developmental stage observed is reported as the lethal point. For da^{GAL4} overexpression, only latest developmental stage reached is reported because the da^{GAL4} stock is not balanced. Overexpression-based phenotypes are scored in greater than 5 larvae or adult flies.

RBBP5 human cDNA rescue evaluation

In human cDNA rescue experiments, $Rbbp5^{Kozak\ GAL4}$ lethality is reported as the latest developmental stage reached. Nonbalanced dead pupae ($n = 19/341$) were observed in self-crosses of $Rbbp5^{Kozak\ GAL4}/TM6B,Sb,Tb$ stocks, and dead larvae were also observed in the crosses. Therefore, there is the possibility that $Rbbp5^{Kozak\ GAL4}$ is lethal at the embryo, larval, and pupal stages; however, for the purposes of this study, rescue was evaluated as the ability of the human cDNA to rescue to the adult developmental stage in ($n > 40$) progeny.

Drosophila developmental staging

The following characteristics were selected to stage animals: early L3 larvae have branched but not extruding spiracles and late L3 larvae have extruding spiracles, visible gut clearance, and exhibit wandering behavior.

Brain immunostaining and brain lobe quantification

For larval counterselection, homozygous da^{GAL4} lines were used and $Actin^{GAL4}$ was crossed to *Cyo, Tb* to create *Actin-GAL4/Cyo,Tb.* These lines were then crossed to homozygous $RBBP5^{Ref}$, $RBBP5^{T232I}$ and $RBBP5^{E296D}$ stocks. Third instar larvae (gut clearance, branched spiracles, and wandering behavior) were dissected in ice-cold PBS. Larval brain preps were fixed in 4% PFA/PBS/2% Triton over-night. Brains were blocked in PBS/2%Triton/5% normal donkey serum for 1 hour. Primary antibodies were incubated overnight; rat anti-Deadpan (Abcam, Cat# ab195173, 1:250) and mouse anti-Prospero (Developmental Studies Hybridoma Bank, Cat# MR1A, 1:1000). Secondary antibodies were incubated for 2 hours at room temperature; rat anti-GFP and mouse anti-Cy3 (1:250). Brains were mounted and imaged using a Zeiss 710 confocal microscope (Neurovisualization core, Baylor College of Medicine) with 1 mm sections. The area of 1 brain lobe was quantified using the area tool in Image J.

Eye area quantification

Whole heads were imaged using a Leica KL1500 LCD microscope using 10× magnification. The area of one eye ($n = 5$) was quantified using the area tool in ImageJ.

Statistical analysis

Statistical analysis was completed using GraphPad prism (Version 9.0.0). Continuous analysis was completed by ordinary one-way ANOVA in which differences between groups were quantified and a P value less than .05 is considered significant.

Results

Identification of individuals and characterization of clinical features

Five unrelated individuals were included in this study. Individual 1 was enrolled in the UDN, subsequently individuals 2 to 5 were identified in unrelated families through GeneMatcher.[21] The 5 individuals presented with neurodevelopmental features, including developmental delay, intellectual disability, and microcephaly. In addition, short stature, musculoskeletal abnormalities, and dysmorphic facies were the common phenotypes observed in this cohort of individuals (Figure 1). Four out of 5 patients were reported to have short stature and microcephaly. Intellectual disability and global developmental delay were seen in all individuals except the youngest. Sensorineural hearing loss and seizure were reported in 2 different individuals. Abnormalities in fingers and toes were observed in all 5 individuals. All individuals presented with dysmorphic facies, but these dysmorphic features did not exhibit as a recognizable pattern. Clinical features of the individuals are summarized in Table 1.

Identification and analysis of variants

All 5 de novo heterozygous variants in *RBBP5* (NM_005057.4) were identified through trio exome or genome sequencing, including 2 missense variants p.(T232I) and p.(E296D) and 3 nonsense/frameshifting variants c.762G>A p.(W254*), c.729del p.(K244Nfs*6), and c.919C>T p.(R307*). *RBBP5* has a pLI score of 1 and missense *z*-score of 4.64,[23,24] suggesting intolerance to haploinsufficiency and missense changes, respectively. In addition, all 5 variants had not been observed in the gno-mAD database (v4.1.0).[2] In silico variant analysis results were inconsistent in their pathogenicity predictions for the missense variants (Supplemental Table 1). Interestingly, all 5 variants are located in a small region between WD40 repeat domains 4 and 6 in *RBBP5.* This region is predicted to be intolerant to changes based on MetaDome analysis, indicating a potential hotspot for pathogenic variants (Figure 2A).[25] The missense variants affect amino acids that are well-conserved across species from human to *Drosophila* (Figure 2B). Expression of the RBBP5 protein with missense variants in HEK293T cells resulted in the full-length protein expressed at a similar level compared with that with a wild-type construct based on western blotting (Figure 2C). However, the single-nucleotide deletion at nucleotide 729 in *RBBP5* p.(K244Nfs*6) produced a frameshift product that terminates prematurely and showed no detectable protein expression. Similarly, the C>T change at nucleotide 919 led to premature termination without protein expression (Figure 2C) confirming that these are complete loss-of-function (null) alleles. In structural analysis of the missense variants, we found that the threonine 232 residue is located in one of the WD40 repeats that mediates the interaction between RBBP5 and the ubiquitinated histone 2B lysine-120 (H2BK120), which has been known to promote the catalytic activity of methyltransferase in H3K4.[26] The p.(T232I) missense variant is predicted to alter the interaction between RBBP5 and the ubiquitinated H2BK120 (Figure 2D and E). Similarly, the E296 residue is located at a crucial position in the loop 2 of RBBP5 WD40 domain, which has been shown to mediate the direct interaction between RBBP5 and the nucleosome.[26] The p.(E296D) variant is expected to affect the conformation of loop 2, which could interfere the binding of RBBP5 to the histones (Figure 2F). Because the missense p.(T232I) and p.(E296D) variants do not affect the protein expression of RBBP5 and structural analysis alone is insufficient to prove the pathogenicity of missense variants, we developed transgenic Drosophila models to investigate the mechanism of these variants in vivo.

Overexpression of human *RBBP5* in *Drosophila* results in microcephaly

For this study, we performed overexpression and rescue experiments with the human *RBBP5* cDNA to determine if the variants have a functional consequence in vivo. The human *RBBP5* is orthologous to *Rbbp5* in *Drosophila* with a high-sequence identity (340/505 amino acids, 67%) and similarity (398/505, 78%) (DIOPT score: 14/16).[27] In flies, *Rbbp5* is a member of the trithorax complex, which is required for differentiation of neural lineages.[28,29] Importantly, neuronal fate determination is similar between humans and flies.[30] Previous research has reported complete loss of H3K4me3 in *Rbbp5* mutant clones.[29] The resulting *Rbbp5* loss-of-function phenotype includes an inability to maintain type II neuroblast identity that gives rise to intermediate progenitor cells. *Rbbp5* null neuroblasts instead express markers for type I neuroblasts.[29] Intermediate progenitor cells undergo several rounds of self-renewal before being committed to a ganglion mother cell

that will terminally differentiate into 2 neurons. Critically, type I neuroblasts are not capable of generating intermediate progenitor cells. This study also demonstrated that neuronal identity and H3K4me3 levels can be restored by the expression of the full-length Rbbp5.[29] A shift from type II to type I neuroblast identity could result in a decrease in the overall number of neurons inducing a microcephaly phenotype in flies, similar to the phenotype of the individuals included in this study.

We first determined whether overexpression of the human reference *RBBP5* cDNA (NM_005057.4) (*RBBP5*^{Ref}) or variants p.(T232I) (*RBBP5*^{T232I}) and p.(E296D) (*RBBP5*^{E296D}) by ubiquitous or tissue-specific *GAL4* drivers cause phenotypes in the fly. In the *GAL4-UAS* system, a *GAL4* transcriptional activator protein is fused to the promoter of a gene of interest. When paired with a construct containing an upstream activation sequence (UAS), this drives expression of the construct based on the spatial and temporal expression pattern of the gene.[31] All *UAS-RBBP5/Rbbp5* lines used in this study are integrated into the same location in the genome to avoid a position effect on expression level.[32] In human protein overexpression paradigms, the endogenous *Drosophila* gene is unaffected, thus enabling the detection of gain- or loss-of-function mechanisms. Gain-of-function variant phenotypes would appear more severe than wild type and complete loss-of-function variants would appear wild type because the fly gene is expressed in the genetic background.[33] Gain-of-function alleles include hyper-, anti-, and neo-morphic alleles in which the variant results in overactive wild-type function or induces dominant negative or novel function in the protein, respectively, as described in previous studies.[34–36] Loss-of-function alleles include hypo- and a-morphic mechanisms that result in a partial or complete loss of protein function, which has been well described in literature.[37–40]

UDN MOSC investigation of candidate variants in the fly has yielded the identification of 59 novel disease genes during phase I of investigation (September 2015-August 2018).[20] We have reported numerous instances in which the overexpression of the human protein results in phenotypes (ie, small eye and wing patterning defects) and confirmed loss-of-function mechanisms as the failure of the variant cDNA to induce the same phenotypes and observed partial loss-of-function as a milder yet still apparent morphological defect.[33,41,42] We have furthermore identified “complex phenotypes” when overexpressing neurodevelopmental risk genes in the fly in which a gain-of-function mechanism is observed in one tissue and a loss-of-function mechanism is observed in another, highlighting the importance of thorough investigation of variant mechanisms.[33] *RBBP5* is located at 1q32.1 and 1q duplication has been identified as a driver of tumorigenesis in breast cancer.[43] Another study identified that *RBBP5* has both high haploinsufficiency and triploinsufficiency scores, which supports a dosage-sensitive mechanism for *RBBP5*.[44] As such, any deviation from wild-type *Rbbp5* (as in the fly) or reference *RBBP5* (as in the human) gene function could be deleterious.

We overexpressed *RBBP5*^{Ref}, *RBBP5*^{T232I}, or *RBBP5*^{E296D} using *Actin-* (*Act-*, strong ubiquitous), *daughterless-* (*da-*, weak ubiquitous) *eyeless-* (*ey-*, developing visual system and parts of the head and brain), *elav-* (neuron), and *repo-* (glia) *GAL4* lines for tissue-specific expression. We then scored lethality by developmental stage in which the *Drosophila* life cycle is 10 days long at 25 °C. Overexpression of *RBBP5*^{Ref} or either missense variant with *Actin*^{GAL4} is lethal in the third instar larval (L3) stage (Figure 3A).

Flies undergo embryo, larval, pupal, and adult stages, and larval development is marked by progression through L1-L3 stages, with L3 spanning 3 days before pupation.[45] Expression of $RBBP5^{Ref}$ with da^{GAL4} is again L3 lethal; however, expression of $RBBP5^{T232I}$ or $RBBP5^{E296D}$ is pupal lethal (Figure 3A). We observe no decrease in viability with *ey-, elav-,* and *repo-GAL4* drivers (Figure 3A). Both *Actin* and *daughterless* are expressed early in development, and these data support previous findings that *Rbbp5* has a critical role early in development. Disruption later in development with *elav-* or $repo^{GAL4}$ induces no phenotype because critical functions have already been carried out when neuronal and glial specific genes are expressed. Importantly, because the fly *Rbbp5* is being expressed in the genetic background in these human cDNA overexpression experiments, observing a loss of larval lethality that is induced by overexpression of the $RBBP5^{Ref}$ suggests that both $RBBP5^{T232I}$ and $RBBP5^{E296D}$ are partial loss-of-function alleles.

We investigated brain development during the larval stage because *daughterless* overexpression of $RBBP5^{Ref}$ is L3 lethal, whereas the expression of $RBBP5^{T232I}$ or $RBBP5^{E296D}$ is pupal lethal. We dissected L3 brains using da^{GAL4} to express a neutral cDNA (da^{GAL4}; *UAS-lacZ*) as an overexpression control and immunostained for markers of progenitor lineages, Deadpan (neuroblasts and intermediate progenitor cells) and Prospero (differentiating neurons)[29] (Figure 3B). Deadpan-positive intermediate progenitor cells are present in the optic lobes of control larvae; however, when $RBBP5^{Ref}$ is expressed, L3 stage-matched brains are severely reduced in size and appear approximately the size of L2 brains with a loss of intermediate progenitor cells in the optic lobes of the brain (Figure 3C and F). Interestingly, although overexpression of either missense variant is pupal lethal, $RBBP5^{T232I}$ and $RBBP5^{E296D}$ L3 brains also fail to develop to control lobe size and are not significantly larger than $RBBP5^{Ref}$ brains (Figure 3D-F) despite the observed difference in lethality staging. These results indicate a discordance between the developmental stage reached (pupa) with the developmental stage of the brain (late L2-early L3) for variant expressing animals and suggest that *RBBP5* could have a pleiotropic effect on growth.

We therefore dissected L3 brains using the strong ubiquitous driver $Actin^{GAL4}$, which induces L3 lethality with $RBBP5^{Ref}$, $RBBP5^{T232I}$, or $RBBP5^{E296D}$. We again performed immunostainings to label neural progenitor lineages with Deadpan and Prospero antibodies.[46] Early and late L3 control ($Actin^{GAL4}$; *UAS-lacZ*) larvae were used to identify neural development occurring throughout the L3 stage (Supplemental Figure 1A and B). Late L3 brains that express $RBBP5^{Ref}$ are less developed in size compared with control stage-matched wandering L3 larva (Supplemental Figure 1C, F). Late L3 brains that express $RBBP5^{T232I}$ or $RBBP5^{E296D}$ also display a small brain (Supplemental Figure 1D-F). Ubiquitous expression of *RBBP5* leads to dramatic reduction in brain size with no significant differences in size between $RBBP5^{Ref}$, $RBBP5^{T232I}$, or $RBBP5^{E296D}$ (Supplemental Figure 1F). Overall, these data suggest that the expression of the human RBBP5 interrupts the function of the fly Rbbp5 protein and results in a strong microcephaly phenotype in the fly.

We also observed changes in overall larval size and development upon ubiquitous overexpression of *RBBP5*. Larval developmental progression is a highly stereotyped pattern and a failure to reach developmental stages indicates possible dysregulation of

factors that direct development.[47] Late L3 larvae ubiquitously expressing *RBBP5*^{Ref}, *RBBP5*^{T232I}, or *RBBP5*^{E296D} with *Actin*^{GAL4} exhibit reduced overall body size compared with control larvae expressing *UAS-lacZ* (Supplemental Figure 2A). Control wandering L3 (Supplemental Figure 2B) develop mature anterior and posterior spiracles indicating that the late L3 stage has been reached.[48] Severe growth phenotypes are seen upon expression of the human reference cDNA. Expression of either *RBBP5*^{Ref} (Supplemental Figure 2C) or *RBBP5*^{T232I} (Supplemental Figure 2D) results mature posterior spiracle formation but failure of the posterior spiracles to develop. In *RBBP5*^{E296D}-expressing larvae, however, anterior and posterior spiracles successfully develop similar to controls (Supplemental Figure 2E). These results indicate an inability of p.(E296D) to induce the developmental phenotype seen in reference expressing larvae again, suggesting a partial loss-of-function mechanism for p.(E296D). To investigate the effect of our *RBBP5* variants on trimethylation in the L3 developmental stage, we confirmed RBBP5 expression with *Actin*^{GAL4} and quantified H3K4me3 compared with total H3 (Supplemental Figure 2F and G). A significant reduction in H3K4me3 is observed compared with *UAS-lacZ* control larvae, whereas no significant change in RBBP5 protein level is observed between *RBBP5*^{Ref}, *RBBP5*^{T232I}, or *RBBP5*^{E296D} (Supplemental Figure 2G). These data confirm that the human RBBP5 can interact with the fly trithorax complex members and that expression of human alleles can affect H3K4me3 levels in the fly. These results also suggest that dysregulation of Rbbp5 results in the failure to express developmental genes that are critical for the progression through the L3 developmental stage.

Tissue-specific *RBBP5* expression in *Drosophila* results in a small eye phenotype

To assess *RBBP5* function in the eye, we drove the variants using the *eyeless*^{GAL4} and quantified eye size in the adult stage. The eyes of *RBBP5*^{Ref} or *RBBP5*^{E296D} flies are smaller than *UAS-lacZ* or *RBBP5*^{T232I} (Figure 4A-E). These data suggest that in the eye, there is a toxic effect of over-expression of *RBBP5*^{Ref}, resulting in a small eye phenotype, and *RBBP5*^{T232I} fails to induce this. Indeed, eye size for *RBBP5*^{T232I} is not significantly smaller than that of the overexpression control (Figure 4E). These results indicate a complete loss-of-function mechanism for p.(T232I) when expressed in a tissue-specific manner in the eye. Overall, these experiments conclude that overexpression of the human *RBBP5* is toxic and results in growth phenotypes, including microcephaly in the brain and reduced size in the body and eye. To summarize these data, we observe both partial and complete loss-of-function mechanisms using overexpression of the human p.(T232I) and p.(E396D) compared with the *RBBP5* reference cDNA. We found partial loss-of-function using ubiquitous overexpression for both missense variants and a complete loss-of-function for p.(T232I) using tissue-specific expression in the eye, suggesting that p.(T232I) could be a stronger hypomorphic allele.

Overexpression of the fly *Rbbp5* induces wing patterning defects

Next, we compared human and fly cDNA overexpression. We generated the orthologous fly *Rbbp5* constructs and created the p.(T232I) and p.(E296D) homologous variants, p.(T231I) (*Rbbp5*^{T231I}) and p.(E295D) (*Rbbp5*^{E295D}), respectively. We compared this with an HA-tagged version of *RBBP5* (*RBBP5-HA*). Ubiquitous expression of *Rbbp5*, *Rbbp5*^{T231I}, or *Rbbp5*^{E295D} with *Actin*^{GAL4} or *da*^{GAL4} is viable, but *Actin*^{GAL4} induces ectopic wing

vein formation that is not fully penetrant at 25°C (Supplemental Figure 3A). Because the GAL4-UAS system is temperature dependent, we increased the culture temperature, and upon expression of *Rbbp5*, ectopic wing vein formation is fully penetrant at 29°C, but the phenotypes of $Rbbp5^{T231I}$ or $Rbbp5^{E295D}$ are not (Supplemental Figure 3B-E). Expression of *RBBP5-HA* is pupal lethal with $Actin^{GAL4}$ and viable with da^{GAL4}, but ectopic wing vein formation is present (Supplemental Figure 3A). Ectopic wing vein formation is observed with both da^{GAL4} and $Actin^{GAL4}$ compared with the laboratory control strain Canton S; however, $Actin^{GAL4}$ escaper flies are rarely observed (Supplemental Figure 3F-H). The ectopic wing vein formation seen upon overexpression of *RBBP5-HA* is similar to the phenotypes observed with *Rbbp5*, suggesting a disruption of factors that direct wing development when the fly or human cDNA is overexpressed. Furthermore, expression of the wild-type fly cDNA induces fully penetrant wing patterning defects, whereas either missense variant p.(T231I) or p.(E295D) results in wing phenotypes that are not fully penetrant, again indicating a partial loss-of-function mechanism in the context of the fly variants.

Rbbp5 is expressed in neurons and glia in the fly brain

To determine the *Rbbp5* expression pattern and further explore the function of the variants, we replaced the open reading frame of *Rbbp5* with the *Kozak GAL4* sequence (*Kozak sequence-GAL4-polyA-FRT-3XP3EGFP-polyA-FRT*).[30] This effectively removes *Rbbp5* and leads to GAL4 expression in a similar spatial and temporal expression pattern (hereafter $Rbbp5^{Kozak\ GAL4}$). The GAL4 transcriptional activator protein will bind UAS-containing constructs to drive expression of a reporter protein or human cDNA to determine if the human protein can rescue loss of the *Drosophila* protein and whether that ability is impaired by the variant.[30] We used the $Rbbp5^{Kozak\ GAL4}$ allele to determine the expression pattern of *Rbbp5* in the developing nervous system. We crossed the $Rbbp5^{Kozak\ GAL4}$ to a *UAS-mCherry NLS* reporter line and determined that *Rbbp5* is expressed in a subset of Elav-positive neurons (Figure 5A-C) and Repo-positive glia (Figure 5D-F) in the optic lobes and ventral nerve cord in the larval brain. Confirming *Rbbp5* expression in both neurons and glia supports the canonical function of *Rbbp5* to direct neuronal fate because type II neuroblasts give rise to both neurons and glia.

RBBP5 missense variants induce a less severe microcephaly phenotype than the human reference cDNA in rescue experiments in an *Rbbp5* null genetic background

Next, we assessed the phenotypes associated with loss of *Rbbp5* function. We dissected L3 brains of $Rbbp5^{Kozak\ GAL4}$ heterozygous mutant animals and a laboratory control strain ($y^1\ w^*$) and again immunostained for markers of progenitor lineages, Deadpan and Prospero.[33] Deadpan-positive intermediate progenitor cells are present in the optic lobes $Rbbp5^{Kozak\ GAL4}$ heterozygous animals (Figure 6A), and there is no difference in brain size between $Rbbp5^{Kozak\ GAL4}$/+ and $y^1\ w^*$ controls (Figure 6F). However, in *Rbbp5* null animals ($Rbbp5^{Kozak\ GAL4}$ / *Df(3L)BSC447*) (*Df(3L)BSC447* is a 125 kB deficiency that encompasses the *Rbbp5* locus), loss of *Rbbp5* is pupal lethal. Furthermore, development of intermediate progenitor cells is severely impaired, and brain size is reduced in the L3 developmental stage (Figure 6B and F). When we attempt to rescue this microcephaly phenotype with $Rbbp5^{Kozak\ GAL4}$-driven expression of $RBBP5^{Ref}$, it fails to rescue the

loss of the fly *Rbbp5*, moreover there is a further reduction in brain size and more severely affected intermediate progenitor cell population (Figure 6C and F). Therefore the $RBBP5^{Ref}$ transgene not only fails to rescue but also exacerbates the loss-of-function phenotypes. Next, we attempted the rescue experiment with $RBBP5^{T232I}$ (Figure 6D) or $RBBP5^{E296D}$ (Figure 6E), and these transgenes also do not rescue, but they do not produce the more severe phenotypes observed with $RBBP5^{Ref}$ (Figure 6C). These results indicate that p.(T232I) or p.(E296D) cannot rescue loss of *Rbbp5* but impair development less severely than the reference cDNA (Figure 6F). This again indicates that overexpression of the $RBBP5^{Ref}$ is toxic and that $RBBP5^{T232I}$ and $RBBP5^{E296D}$ are less toxic even when expressed under the control of endogenous *Rbbp5* promoter. In summary, total brain lobe area was reduced in the *Rbbp5* mutants and was not rescued by the human reference nor the p.(T232I) or p.(E296D) transgenes. However, $RBBP5^{Ref}$ produces even stronger lobe size reduction than *Rbbp5* null larvae. Furthermore, there is no significant difference in brain lobe area between either $RBBP5^{T232I}$ or $RBBP5^{E296D}$ in a null genetic background and *RBBP5* null lobe size, again supporting the finding that p.(T232I) and p.(E296D) are loss-of-function alleles (Figure 6F). This is consistent with the phenotypes observed in overexpression experiments with $RBBP5^{T232I}$ and $RBBP5^{E296D}$ failing to induce the toxic effects of $RBBP5^{Ref}$. Ubiquitous expression of $RBBP5^{Ref}$ induces earlier lethality than expression of $RBBP5^{T232I}$ or $RBBP5^{E296D}$, and impaired growth phenotypes are present upon expression of the human *RBBP5* reference that are not present when the missense variants are expressed indicating a hypomorphic loss-of-function mechanism for the p.(T232I) and p.(E296D) variants. Experimental findings supporting a loss-of-function mechanism for p.(T232I) and p.(E296D) are summarized in Supplemental Table 2.

Discussion

In this study, we identified 5 affected individuals with de novo heterozygous variants in one of the COMPASS core members *RBBP5*. We propose that haploinsufficient loss of *RBBP5* is responsible for the neurodevelopmental disorder presented here. This is consistent with the fact that *RBBP5* has a pLI score of 1, and other disorders of epigenetic machinery classically are due to haploinsufficiency.[5] We confirm that the frameshifting/nonsense variants are loss-of-function null alleles. Additionally, the p.(T232I) and p.(E296D) missense variants also meet the criteria for a pathogenic variant based on the variant interpretation guidelines from a joint consensus recommendation of the American College of Medical Genetics and Genomics and the Association for Molecular Pathology.[49] These criteria include confirmed de novo variants, in vitro or in vivo functional studies supportive of a damaging effect, the absence of these variants in the population database, and the low rate of benign missense variation in *RBBP5* (Supplemental Table 1). We have also conducted a search in a large clinical exome/genome database at Baylor Genetics for candidate *RBBP5* variants, which identified 2 likely benign de novo variants. These 2 cases were considered as likely benign because of inconsistent phenotype and benign in silico analysis (Supplemental Tables 1 and 3).

The COMPASS protein complex consists of 4 core members: RBBP5, WDR5, ASH2L, and 1 of the 6 methyltransferases.[50] The methyltransferases have the enzymatic SET1 domain to methylate H3K4, whereas RBBP5 functions to modulate the activity of the complex

and mediate the interaction between the nucleosome and the complex.[4,51] Our structural analysis showed both the T232 and E296 residues are located at critical positions of the interface between RBBP5 and the histones, which has been known to be involved in the recruitment of COMPASS to the nucleosome and promoting the methyltransferase activity in H3K4.[26,52,53] The mutations in T232 and E296 are likely to interrupt the interaction between RBBP5 and histones, resulting in the dysregulation of downstream target genes.

Kabuki syndrome is one of the most common disorders in the epigenetic machinery.[6] *KMT2D*, one of the methyltransferases in the COMPASS, is the major disease gene for the Kabuki syndrome. Nevertheless, about 20% to 30% of clinically diagnosed Kabuki syndrome patients have negative genetic testing.[6] It has been hypothesized that a pathogenic variant in other COMPASS members could result in a disorder that phenotypically resembles Kabuki syndrome.[7] We observe some striking similarities in phenotypes between our probands and those typically seen in patients with Kabuki syndrome, such as the neurodevelopmental features, microcephaly, short stature, hypotonia, sensorineural hearing loss, and seizure.[54] However, there are phenotypes such as congenital cardiac defects and the characteristic dysmorphic facial features in the Kabuki syndrome that are absent in our probands. Given KMT2D is only 1 of the 6 methyltransferases to which RBBP5 binds, it is reasonable to expect differences in the clinical spectrum between *KMT2D*- and *RBBP5*-related disorders.

The *Drosophila* model has previously been used to confirm the functional mechanism of variants in SET domain-containing methyltransferases.[55] The fly Rbbp5 interacts with trithorax proteins, a coactivator complex that maintains gene activation through H3K4 methylation.[28] The Kabuki syndrome implicated methyltransferase *KMT2D* is homologous to *trithorax related* (*trr*), a gene that is important for eye development and hormone responsive development.[56] In addition to RBBP5, another COMPASS member ASH2L homolog, ash2, also interacts with Trr and the ecdysone receptor (EcR) to direct molting and metamorphosis.[57] Notably, *ash2* mutants also exhibit neural and optic lobe developmental defects.[58]

We present evidence that the *RBBP5* p.(T232I) and p.(E296D) variants are hypomorphic loss-of-function alleles. We observed earlier lethality upon ubiquitous expression of the human reference than either missense variant (Figure 3). We also observed variant-specific loss-of-function phenotypes using ubiquitous and tissue-specific overexpression (Figure 4, Supplemental Figure 2). We identified that *Rbbp5* is expressed in both neurons and glia in the developing *Drosophila* brain (Figure 5). We found that loss of *Rbbp5* results in microcephaly in the larval stage and confirmed that this loss is lethal (Figure 6). Unfortunately, the human *RBBP5* is unable to rescue loss of the *Drosophila Rbbp5* gene. Failure to rescue with the human cDNA is observed in 30% of cases in our experience. The human protein may bind different targets or could have less specificity at the lower body temperature of flies or other reasons stemming from evolutionary divergence. This could also be influenced by the precise expression of neural genes that is required for brain development. Indeed, we observe consistent microcephaly phenotypes across all genotypes, even when overall body size is not as severely affected (Supplemental Figures 1 and 2). However, we did find variant-specific differences when the *RBBP5* transgenes

are expressed. A similar microcephaly phenotype is induced upon co-expression of either p.(T232I) or p.(E296D) in an *Rbbp5* null background that is not as severe as co-expression of the human reference. Moreover, expression of p.(T232I) or p.(E296D) in a null background induces the same microcephaly phenotype as seen in *Rbbp5* null animals confirming that both missense variants are loss-of-function alleles (see Figure 6). In addition, expression of the fly and human cDNA leads to wing patterning defects, and expression of the fly p.(T231I) or p.(E295D) variants fail to induce fully penetrant wing patterning defects as seen upon overexpression of the fly *Rbbp5* (Supplemental Figure 3). We observe both complete and partial loss-of-function phenotypes through analysis of the p.(T232I) and p.(E296D) variants using the human cDNA (Supplemental Table 2). Thus, a conservative evaluation is that they are partial loss-of-function alleles. Because we do not observe milder phenotypes in clinical symptoms between missense and truncating variants, we cannot exclude that these variants could be complete loss-of-function alleles in the human system. From these cumulative data, we conclude that both missense variants investigated in this study are partial loss-of-function hypomorphic alleles.

We have shown that H3K4 trimethylation is disrupted in *RBBP5* expressing animals, suggesting an inability to activate expression of key developmental genes. We observed variant-specific developmental abnormalities in larvae ubiquitously overexpressing *RBBP5*, including microcephaly and overall growth phenotypes. Therefore, the p.(T232I) and p.(E296D) variants disrupt the function of the COMPASS complex possibly because of the substitution of critical residues, resulting in an inability to trimethylate H3K4 to direct downstream transcriptional activation. Because we observe unique tissue-specific loss-of-function phenotypes between the missense variants, it is possible that downstream gene expression is dysregulated in a variant-specific manner. Future transcriptomics studies could identify the critical genes dysregulated by these and additional *RBBP5* variants. Furthermore, inclusion of variants in additional members of the COMPASS complex in transcriptomics studies could begin to identify the target genes responsible for the overlapping and distinct phenotypes involved in the spectrum of observed clinical symptoms.

In summary, we have provided the first evidence for a syndromic neurodevelopmental disorder that is associated with pathogenic variants in *RBBP5*. This study provides a new perspective to the disorders of the epigenetic machinery.

Supplementary Material

Refer to Web version on PubMed Central for supplementary material.

Acknowledgments

The authors thank all participating patients and their family members for supporting this study.

Funding

This research was funded by UDN UCLA clinical site grant 2U01HG007703 to J.A.M.-A., S.F.N., and C.G.P. and UDN model organism screening center grant U54 NS093793 to M.F.W., S.Y., and H.J.B. This work was partially supported by programs of the California Center for Rare Diseases, UCLA Institute of Precision Health, and a

NIGMS T32 training grant to Y.H. (5T32GM008243). The content is solely the responsibility of the authors and does not necessarily represent the official views of the National Institutes of Health.

Data Availability

The authors confirm that the data supporting the findings of this research are available within the manuscript or available upon request.

References

1. Jambhekar A, Dhall A, Shi Y. Roles and regulation of histone methylation in animal development. Nat Rev Mol Cell Biol. 2019;20(10):625–641. 10.1038/s41580-019-0151-1 [PubMed: 31267065]
2. Douillet D, Sze CC, Ryan C, et al. Uncoupling histone H3K4 trimethylation from developmental gene expression via an equilibrium of COMPASS, Polycomb and DNA methylation. Nat Genet. 2020;52(6):615–625. 10.1038/s41588-020-0618-1 [PubMed: 32393859]
3. Hu D, Gao X, Cao K, et al. Not All H3K4 methylations are created equal: Mll2/COMPASS dependency in primordial germ cell specification. Mol Cell. 2017;65:460–475.e6. 10.1016/j.molcel.2017.01.013 [PubMed: 28157506]
4. Han J, Li T, Li Y, et al. The internal interaction in RBBP5 regulates assembly and activity of MLL1 methyltransferase complex. Nucleic Acids Res. 2019;47(19):10426–10438. 10.1093/nar/gkz819 [PubMed: 31544921]
5. Fahrner JA, Bjornsson HT. Mendelian disorders of the epigenetic machinery: postnatal malleability and therapeutic prospects. Hum Mol Genet. 2019;28(R2):R254–R264. 10.1093/hmg/ddz174 [PubMed: 31595951]
6. Lintas C, Persico AM. Unraveling molecular pathways shared by Kabuki and Kabuki-like syndromes. Clin Genet. 2018;94(3–4):283–295. 10.1111/cge.12983 [PubMed: 28139835]
7. Adam M Insights into the molecular genetics of Kabuki syndrome. Adv Genomics Genet. 2015;5:121–129. 10.2147/AGG.S58588
8. Ramoni RB, Mulvihill JJ, Adams DR, et al. The undiagnosed diseases network: accelerating discovery about health and disease. Am J Hum Genet. 2017;100(2):185–192. 10.1016/j.ajhg.2017.01.006 [PubMed: 28157539]
9. Gahl WA, Mulvihill JJ, Toro C, et al. The NIH Undiagnosed Diseases Program and Network: applications to modern medicine. Mol Genet Metab. 2016;117(4):393–400. 10.1016/j.ymgme.2016.01.007 [PubMed: 26846157]
10. Splinter K, Adams DR, Bacino CA, et al. Effect of genetic diagnosis on patients with previously undiagnosed disease. N Engl J Med. 2018;379(22):2131–2139. 10.1056/NEJMoa1714458 [PubMed: 30304647]
11. Wangler MF, Yamamoto S, Chao HT, et al. Model organisms facilitate rare disease diagnosis and therapeutic research. Genetics. 2017;207(1):9–27. 10.1534/genetics.117.203067 [PubMed: 28874452]
12. Bellen HJ, Wangler MF, Yamamoto S. The fruit fly at the interface of diagnosis and pathogenic mechanisms of rare and common human diseases. Hum Mol Genet. 2019;28(R2):R207–R214. 10.1093/hmg/ddz135 [PubMed: 31227826]
13. Kanca O, Bellen HJ, Schnorrer F. Gene tagging strategies to assess protein expression, localization, and function in Drosophila. Genetics. 2017;207(2):389–412. 10.1534/genetics.117.199968 [PubMed: 28978772]
14. Lee PT, Zirin J, Kanca O, et al. A gene-specific T2A-GAL4 library for Drosophila. Elife. 2018;7:e35574. 10.7554/eLife.35574 [PubMed: 29565247]
15. Kanca O, Zirin J, Garcia-Marques J, et al. An efficient CRISPR-based strategy to insert small and large fragments of DNA using short homology arms. eLife. 2019;8:e35574. 10.7554/eLife.51539
16. Harnish JM, Deal SL, Chao HT, Wangler MF, Yamamoto S. In vivo functional study of disease-associated rare human variants using Drosophila. J Vis Exp. 2019;150:10.3791/59658. 10.3791/59658.

17. Baxter SM, Posey JE, Lake NJ, et al. Centers for Mendelian genomics: a decade of facilitating gene discovery. Genet Med. 2022;24(4):784–797. 10.1016/j.gim.2021.12.005 [PubMed: 35148959]
18. Liu P, Meng L, Normand EA, et al. Reanalysis of clinical exome sequencing data. N Engl J Med. 2019;380(25):2478–2480. 10.1056/NEJMc1812033 [PubMed: 31216405]
19. Posey JE, O'Donnell-Luria AH, Chong JX, et al. Insights into genetics, human biology and disease gleaned from family based genomic studies. Genet Med. 2019;21(4):798–812. 10.1038/s41436-018-0408-7 [PubMed: 30655598]
20. Baldridge D, Wangler MF, Bowman AN, et al. Model organisms contribute to diagnosis and discovery in the undiagnosed diseases network: current state and a future vision. Orphanet J Rare Dis. 2021;16(1):206. 10.1186/s13023-021-01839-9 [PubMed: 33962631]
21. Sobreira N, Schiettecatte F, Valle D, Hamosh A. GeneMatcher: a matching tool for connecting investigators with an interest in the same gene. Hum Mutat. 2015;36(10):928–930. 10.1002/humu.22844 [PubMed: 26220891]
22. Kanca O, Zirin J, Hu Y, et al. An expanded toolkit for Drosophila gene tagging using synthesized homology donor constructs for CRISPR-mediated homologous recombination. Elife. 2022;11:e76077. 10.7554/eLife.76077 [PubMed: 35723254]
23. Karczewski KJ, Francioli LC, Tiao G, et al. The mutational constraint spectrum quantified from variation in 141,456 humans. Nature. 2020;581(7809):434–443. 10.1038/s41586-020-2308-7 [PubMed: 32461654]
24. Wang J, Al-Ouran R, Hu Y, et al. MARRVEL: integration of human and model organism genetic resources to facilitate functional annotation of the human genome. Am J Hum Genet. 2017;100(6):843–853. 10.1016/j.ajhg.2017.04.010 [PubMed: 28502612]
25. Wiel L, Baakman C, Gilissen D, Veltman JA, Vriend G, Gilissen C. MetaDome: pathogenicity analysis of genetic variants through aggregation of homologous human protein domains. Hum Mutat. 2019;40(8):1030–1038. 10.1002/humu.23798 [PubMed: 31116477]
26. Xue H, Yao T, Cao M, et al. Structural basis of nucleosome recognition and modification by MLL methyltransferases. Nature. 2019;573(7774):445–449. 10.1038/s41586-019-1528-1 [PubMed: 31485071]
27. Hu Y, Flockhart I, Vinayagam A, et al. An integrative approach to ortholog prediction for disease-focused and other functional studies. BMC Bioinformatics. 2011;12:357. 10.1186/1471-2105-12-357 [PubMed: 21880147]
28. Schuettengruber B, Bourbon HM, Di Croce L, Cavalli G. Genome regulation by Polycomb and trithorax: 70 years and counting. Cell. 2017;171(1):34–57. 10.1016/j.cell.2017.08.002 [PubMed: 28938122]
29. Komori H, Xiao Q, Janssens DH, Dou Y, Lee CY. Trithorax maintains the functional heterogeneity of neural stem cells through the transcription factor buttonhead. Elife. 2014;3:e03502. 10.7554/eLife.03502 [PubMed: 25285447]
30. Kim DW, Hirth F. Genetic mechanisms regulating stem cell self-renewal and differentiation in the central nervous system of Drosophila. Cell Adh Migr. 2009;3(4):402–411. 10.4161/cam.3.4.8690 [PubMed: 19421003]
31. Brand AH, Perrimon N. Targeted gene expression as a means of altering cell fates and generating dominant phenotypes. Development. 1993;118(2):401–415. 10.1242/dev.118.2.401 [PubMed: 8223268]
32. Venken KJT, He Y, Hoskins RA, Bellen HJ. P[acman]: a BAC transgenic platform for targeted insertion of large DNA fragments in D melanogaster. Science. 2006;314(5806):1747–1751. 10.1126/science.1134426 [PubMed: 17138868]
33. Marcogliese PC, Deal SL, Andrews J, et al. Drosophila functional screening of de novo variants in autism uncovers damaging variants and facilitates discovery of rare neurodevelopmental diseases. Cell Rep. 2022;38(11):110517. 10.1016/j.celrep.2022.110517 [PubMed: 35294868]
34. Luo X, Rosenfeld JA, Yamamoto S, et al. Clinically severe CACNA1A alleles affect synaptic function and neurodegeneration differentially. PLoS Genet. 2017;13(7):e1006905. 10.1371/journal.pgen.1006905 [PubMed: 28742085]

35. Chung HL, Wangler MF, Marcogliese PC, et al. Loss- or gain-of-function mutations in ACOX1 cause axonal loss via different mechanisms. Neuron. 2020;106(4):589–606.e6. 10.1016/j.neuron.2020.02.021 [PubMed: 32169171]
36. Luo X, Schoch K, Jangam SV, et al. Rare deleterious de novo missense variants in Rnf2/Ring2 are associated with a neurodevelopmental disorder with unique clinical features. Hum Mol Genet. 2021;30(14):1283–1292. 10.1093/hmg/ddab110 [PubMed: 33864376]
37. Link N, Chung H, Jolly A, et al. Mutations in ANKLE2, a ZIKA virus target, disrupt an asymmetric cell division pathway in drosophila neuroblasts to cause microcephaly. Dev Cell. 2019;51(6):713–729.e6. 10.1016/j.devcel.2019.10.009 [PubMed: 31735666]
38. Marcogliese PC, Dutta D, Ray SS, et al. Loss of IRF2BPL impairs neuronal maintenance through excess Wnt signaling. Sci Adv. 2022;8(3):eabl5613. 10.1126/sciadv.abl5613 [PubMed: 35044823]
39. Guo H, Bettella E, Marcogliese PC, et al. Disruptive mutations in TANC2 define a neurodevelopmental syndrome associated with psychiatric disorders. Nat Commun. 2019;10(1):4679. 10.1038/s41467-019-12435-8 [PubMed: 31616000]
40. Ravenscroft TA, Phillips JB, Fieg E, et al. Heterozygous loss-of-function variants significantly expand the phenotypes associated with loss of GDF11. Genet Med. 2021;23(10):1889–1900. 10.1038/s41436-021-01216-8 [PubMed: 34113007]
41. Liu N, Schoch K, Luo X, et al. Functional variants in TBX2 are associated with a syndromic cardiovascular and skeletal developmental disorder. Hum Mol Genet. 2018;27(14):2454–2465. 10.1093/hmg/ddy146 [PubMed: 29726930]
42. Goodman LD, Cope H, Nil Z, et al. TNPO2 variants associate with human developmental delays, neurologic deficits, and dysmorphic features and alter TNPO2 activity in Drosophila. Am J Hum Genet. 2021;108(9):1669–1691. 10.1016/j.ajhg.2021.06.019 [PubMed: 34314705]
43. Privitera AP, Barresi V, Condorelli DF. Aberrations of chromosomes 1 and 16 in breast cancer: a framework for cooperation of transcriptionally dysregulated genes. Cancers (Basel). 2021;13(7):1585. 10.3390/cancers13071585 [PubMed: 33808143]
44. Collins RL, Glessner JT, Porcu E, et al. A cross-disorder dosage sensitivity map of the human genome. Cell. 2022;185(16):3041–3055. e25. 10.1016/j.cell.2022.06.036 [PubMed: 35917817]
45. Ong C, Yung LYL, Cai Y, Bay BH, Baeg GH. Drosophila melanogaster as a model organism to study nanotoxicity. Nanotoxicology. 2015;9(3):396–403. 10.3109/17435390.2014.940405 [PubMed: 25051331]
46. San-Juán BP, Baonza A. The bHLH factor deadpan is a direct target of Notch signaling and regulates neuroblast self-renewal in Drosophila. Dev Biol. 2011;352(1):70–82. 10.1016/j.ydbio.2011.01.019 [PubMed: 21262215]
47. Tennessen JM, Thummel CS. Coordinating growth and maturation – insights from Drosophila. Curr Biol. 2011;21(18):R750–R757. 10.1016/j.cub.2011.06.033 [PubMed: 21959165]
48. Hu N, Castelli-Gair J. Study of the posterior spiracles of Drosophila as a model to understand the genetic and cellular mechanisms controlling morphogenesis. Dev Biol. 1999;214(1):197–210. 10.1006/dbio.1999.9391 [PubMed: 10491268]
49. Richards S, Aziz N, Bale S, et al. Standards and guidelines for the interpretation of sequence variants: a joint consensus recommendation of the American College of Medical Genetics and Genomics and the Association for Molecular Pathology. Genet Med. 2015;17(5):405–424. 10.1038/gim.2015.30 [PubMed: 25741868]
50. Namitz KEW, Showalter SA, Cosgrove MS. Phase separation promotes a highly active oligomeric scaffold of the MLL1 core complex for regulation of histone H3K4 methylation. J Biol Chem. 2023;299(10):105204. 10.1016/j.jbc.2023.105204 [PubMed: 37660926]
51. Cao F, Chen Y, Cierpicki T, et al. An Ash2L/RbBP5 heterodimer stimulates the MLL1 methyltransferase activity through coordinated substrate interactions with the MLL1 SET domain. PLoS One. 2010;5(11):e14102. 10.1371/journal.pone.0014102 [PubMed: 21124902]
52. Park SH, Ayoub A, Lee YT, et al. Cryo-EM structure of the human MLL1 core complex bound to the nucleosome. Nat Commun. 2019;10(1):5540. 10.1038/s41467-019-13550-2 [PubMed: 31804488]

53. Kwon M, Park K, Hyun K, et al. H2B ubiquitylation enhances H3K4 methylation activities of human KMT2 family complexes. Nucleic Acids Res. 2020;48(10):5442–5456. 10.1093/nar/gkaa317 [PubMed: 32365172]

54. Adam MP, Banka S, Bjornsson HT, et al. Kabuki syndrome: international consensus diagnostic criteria. J Med Genet. 2019;56(2):89–95. 10.1136/jmedgenet-2018-105625 [PubMed: 30514738]

55. Jangam SV, Briere LC, Jay KL, et al. A de novo missense variant in EZH1 associated with developmental delay exhibits functional deficits in Drosophila melanogaster. Genetics. 2023;224(4):iyad110. 10.1093/genetics/iyad110

56. Sedkov Y, Cho E, Petruk S, et al. Methylation at lysine 4 of histone H3 in ecdysone-dependent development of Drosophila. Nature. 2003;426(6962):78–83. 10.1038/nature02080 [PubMed: 14603321]

57. Carbonell A, Mazo A, Serras F, Corominas M. Ash2 acts as an ecdysone receptor coactivator by stabilizing the histone methyltransferase Trr. Mol Biol Cell. 2013;24(3):361–372. 10.1091/mbc.E12-04-0267 [PubMed: 23197473]

58. Beltran S, Blanco E, Serras F, et al. Transcriptional network controlled by the trithorax-group gene ash2 in Drosophila melanogaster. Proc Natl Acad Sci U S A. 2003;100(6):3293–3298. 10.1073/pnas.0538075100 [PubMed: 12626737]

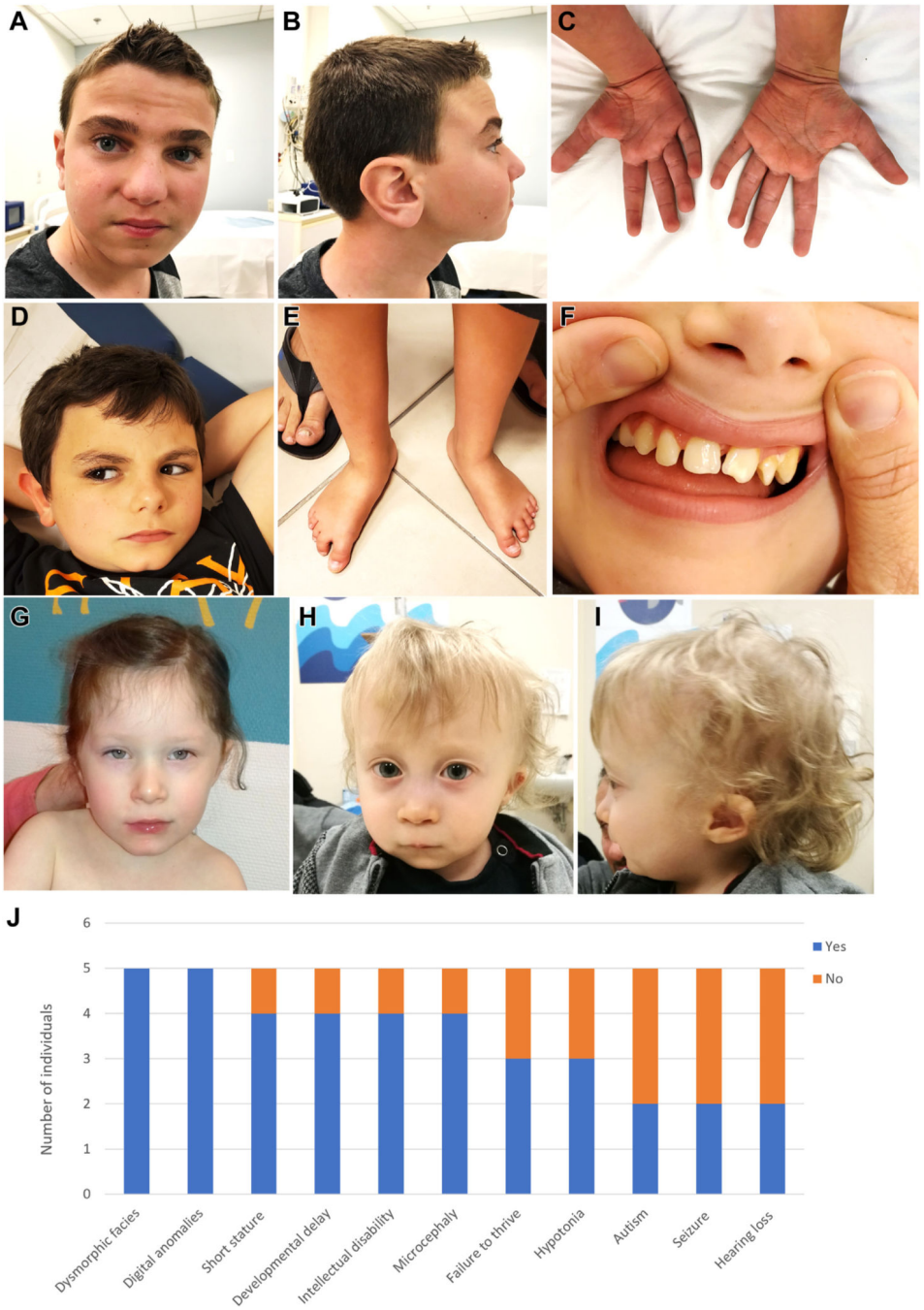

Figure 1. Human subjects with *RBBP5* de novo variants exhibit a range of clinical features.

Dysmorphic features in individual 1, including hypertelorism, high arched eyebrow, long eyelashes, synophrys, and board nasal tip as shown in (A); retrognathia, large ear, and a preauricular ear tag as shown in (B); bilateral 5th finger clinodactyly and prominent fingertip pad in (C). Dysmorphic features in individual 3 as shown in (D) with midface hypoplasia and cupped ears, clinodacyly in (E), and supernumerary teeth in (F). Dysmorphic features in individual 4 as shown in (G) with short and upslanting palpebral fissures, high forehead, anteverted nostrils, and sparse eyebrows. (H) and (I) shows the dysmorphic facial features,

including sparse eyebrows, short nose, long philtrum, small and squared ears, and small mouth with thin lips, in individual 5. Common phenotypes are illustrated in (J).

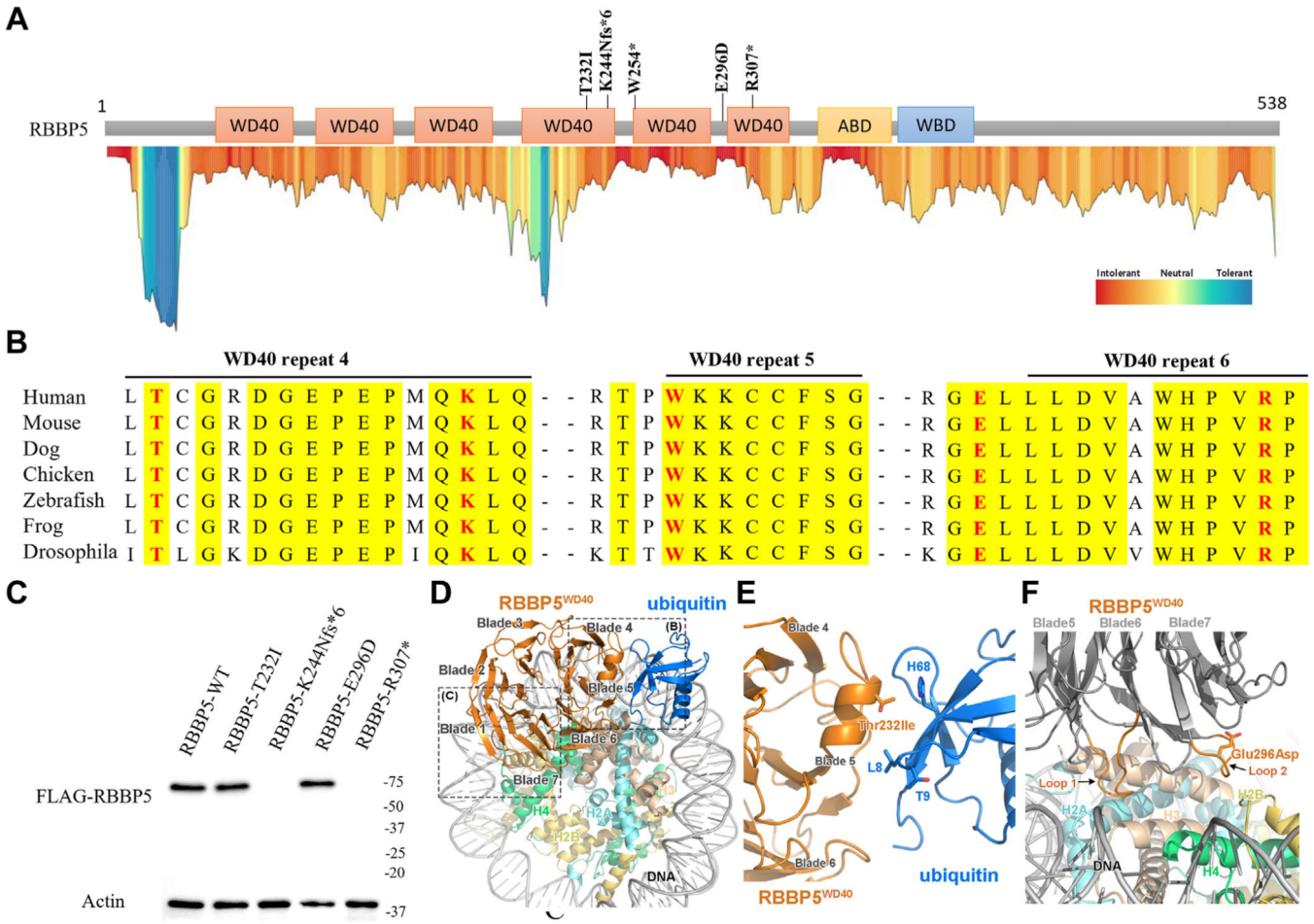

Figure 2. Bioinformatic and structural variant analysis.

The functional domains of RBBP5 and position of variants in MetaDome are shown in (A). The evolutionarily conserved residues affected by variants are shown in (B). The protein expression of FLAG-tagged human RBBP5 reference and variants were shown in (C). Structure analysis of T232 and E296 were performed in RBBP5^{WD40} of the cryo-EM structure of MLL3-ubNCP complex. The overall structure of RBBP5^{WD40} complexed with a nucleosome core particle mono-ubiquitinated at the Lys 120 of histone H2B (ubNCP). The RBBP5 WD40 repeat 4 is sandwiched between ubiquitin and core histones. The RBBP5^{WD40} is shown in orange and ubiquitin in blue (D). Detailed view of the recognition interface of RBBP5^{WD40}-ubiquitin. Residue p.(T232I), which is located on the α-helix-containing loop of RBBP5^{WD40} blade 5, lies close to residues L8, T9, and H68 of ubiquitin (E). All these residues are shown in stick model. Detailed view of the interaction interface between RBBP5^{WD40} and histone H2B-H4. Two loops (loop 1 and loop 2), which connect the WD40 propeller blades 5, 6, and 7, interact with nucleosome directly. Residue p.(E296D) is located on loop 2 and shown in stick model (F).

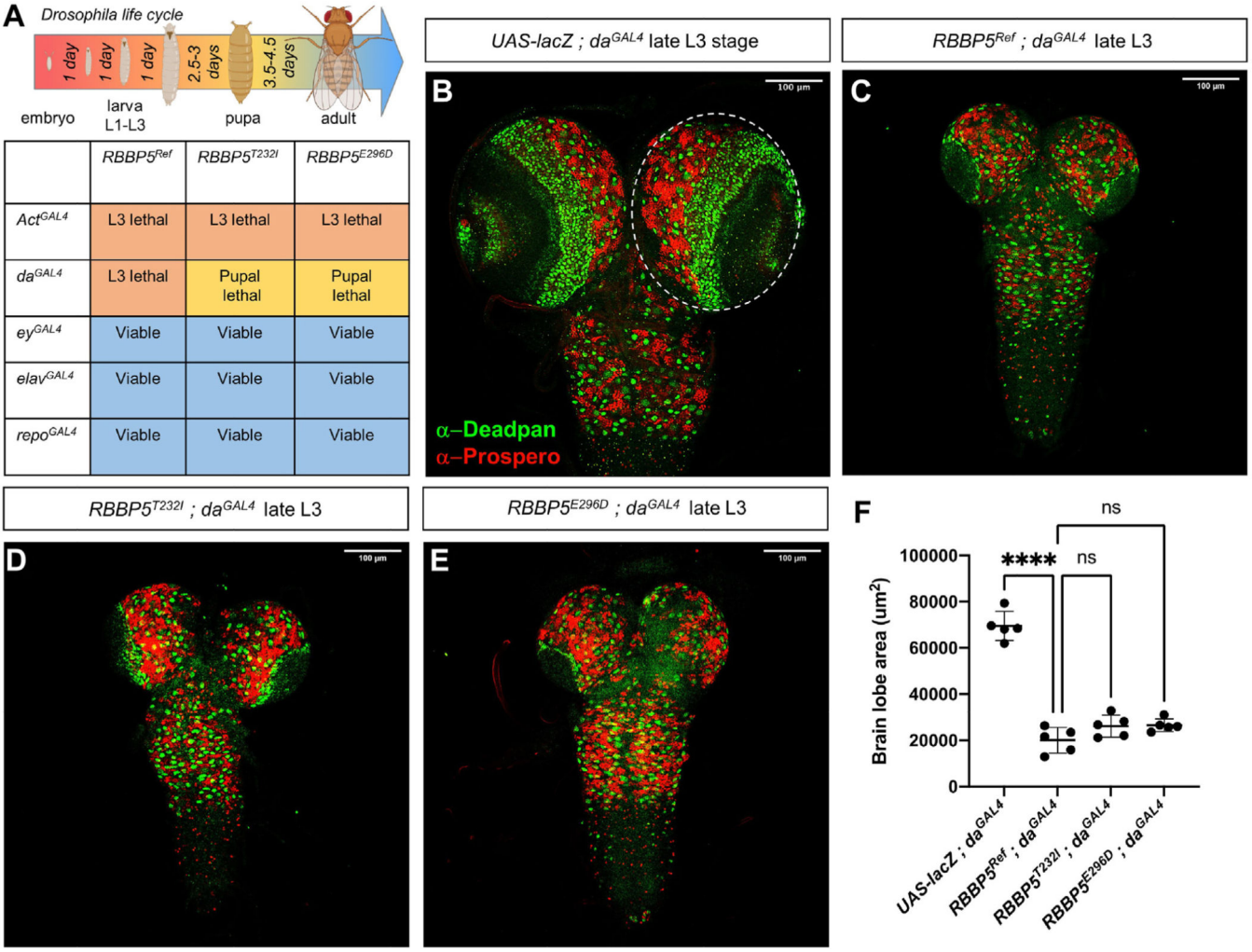

	$RBBP5^{Ref}$	$RBBP5^{T232I}$	$RBBP5^{E296D}$
Act^{GAL4}	L3 lethal	L3 lethal	L3 lethal
da^{GAL4}	L3 lethal	Pupal lethal	Pupal lethal
ey^{GAL4}	Viable	Viable	Viable
$elav^{GAL4}$	Viable	Viable	Viable
$repo^{GAL4}$	Viable	Viable	Viable

Figure 3. Ubiquitous expression of *RBBP5* in flies induces lethality and results in microcephaly in the larval developmental stage.

The *Drosophila* life cycle is approximately 10 days long at 25°C. Expression of the human *RBBP5* or either missense variant with a strong ubiquitous driver ($Actin^{GAL4}$) is larval lethal ($Actin^{GAL4}$ / $RBBP5^{Ref}$ observed in 0/128 F1 progeny, o/e 0.0; $Actin^{GAL4}/RBBP5^{T232I}$ observed in 0/144 F1 progeny, o/e 0.0; $Actin^{GAL4}/RBBP5^{E296D}$ observed in 0/277, o/e 0.0). With a weak ubiquitous driver (da^{GAL4}), expression of the human reference is larval lethal, but expression of p.(T232I) or p.(E296D) is pupal lethal. Expression with tissue specific (*ey*-, *elav*-, or $repo^{GAL4}$) drivers does not affect viability in (A). Representative developmentally staged control late L3 brains (*UAS-lacZ;* da^{GAL4}) with Deadpan staining of neuroblasts and intermediate progenitor cells in green and Prospero staining of neural progenitors in red in (B). Experimental *RBBP5* reference ($RBBP5^{Ref}$; da^{GAL4}) brain shown in (C), $RBBP5^{T232I}$ ($RBBP5^{T232I}$; da^{GAL4}) in (D) and $RBBP5^{E296D}$ ($RBBP5^{E296D}$; da^{GAL4}) in (E). Quantification of ubiquitous overexpression (da^{GAL4}) of $RBBP5^{Ref}$, $RBBP5^{T232I}$, and $RBBP5^{E296D}$ compared with *UAS-lacZ* (one-way ANOVA, ns, $P > .05$, $*P < .05$, $**P < .01$, $***P < .001$, $****P < .0001$) in (F). Created with Biorender.com.

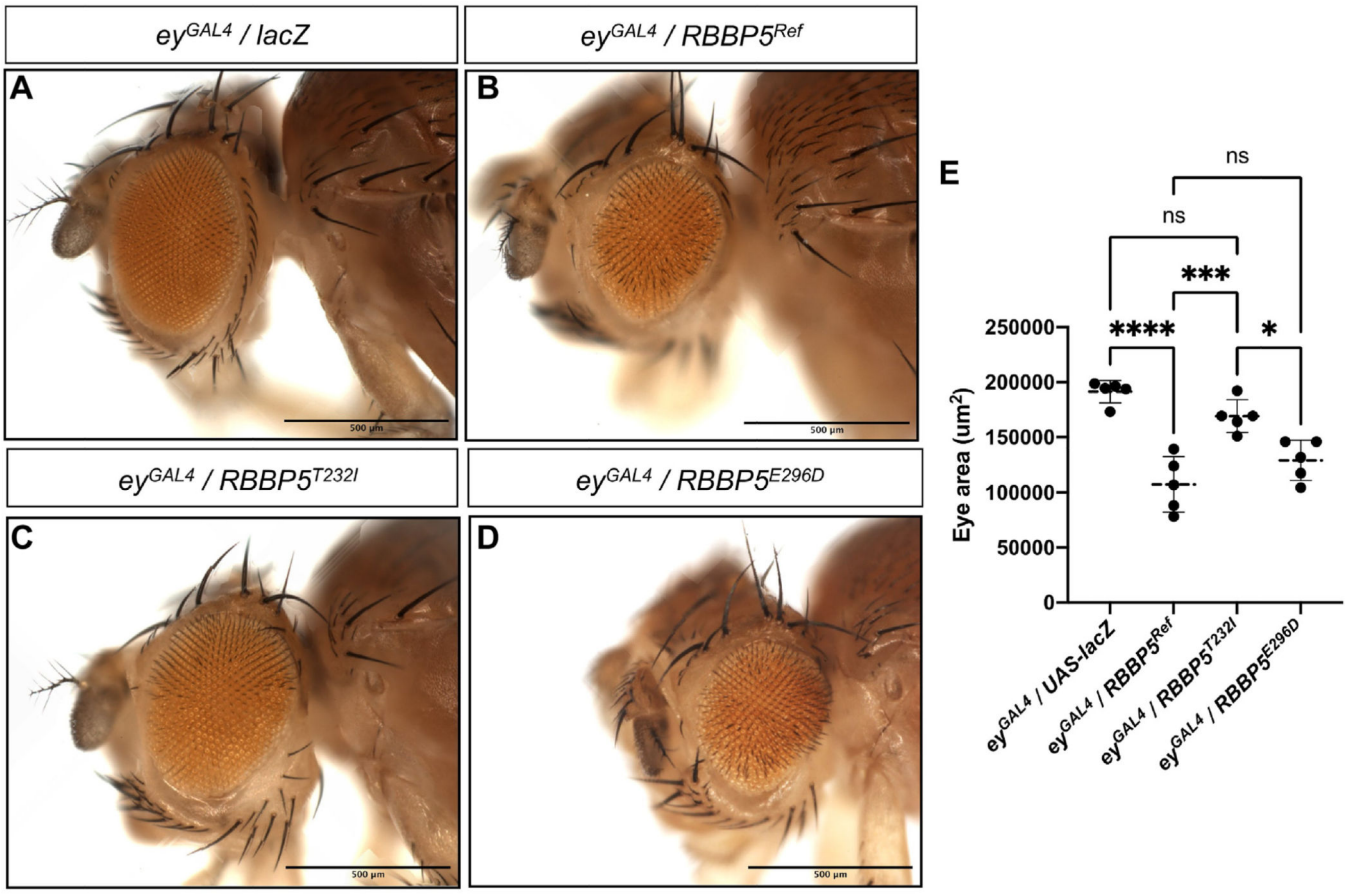

Figure 4. Human *RBBP5* expression induces a small eye phenotype not recapitulated by the p.(T232I) variant.

Overexpression with *eyeless-GAL4* (ey^{GAL4}) in a control line (ey^{GAL4} / *UAS-lacZ*) as shown in (A), ey^{GAL4} / $RBBP5^{Ref}$ in (B), ey^{GAL4} / $RBBP5^{T232I}$ in (C), and ey^{GAL4} / $RBBP5^{E296D}$ in (D). Expression of $RBBP5^{Ref}$ and $RBBP5^{E296D}$ results in a small eye phenotype compared with *UAS-lacZ*. Expression of $RBBP5^{T232I}$ does not induce a small eye phenotype and eye size is not significantly different than controls (one-way ANOVA, ns $P > .05$, * $P < .05$, ** $P < .01$, *** $P < .001$, **** $P < .0001$) in (E).

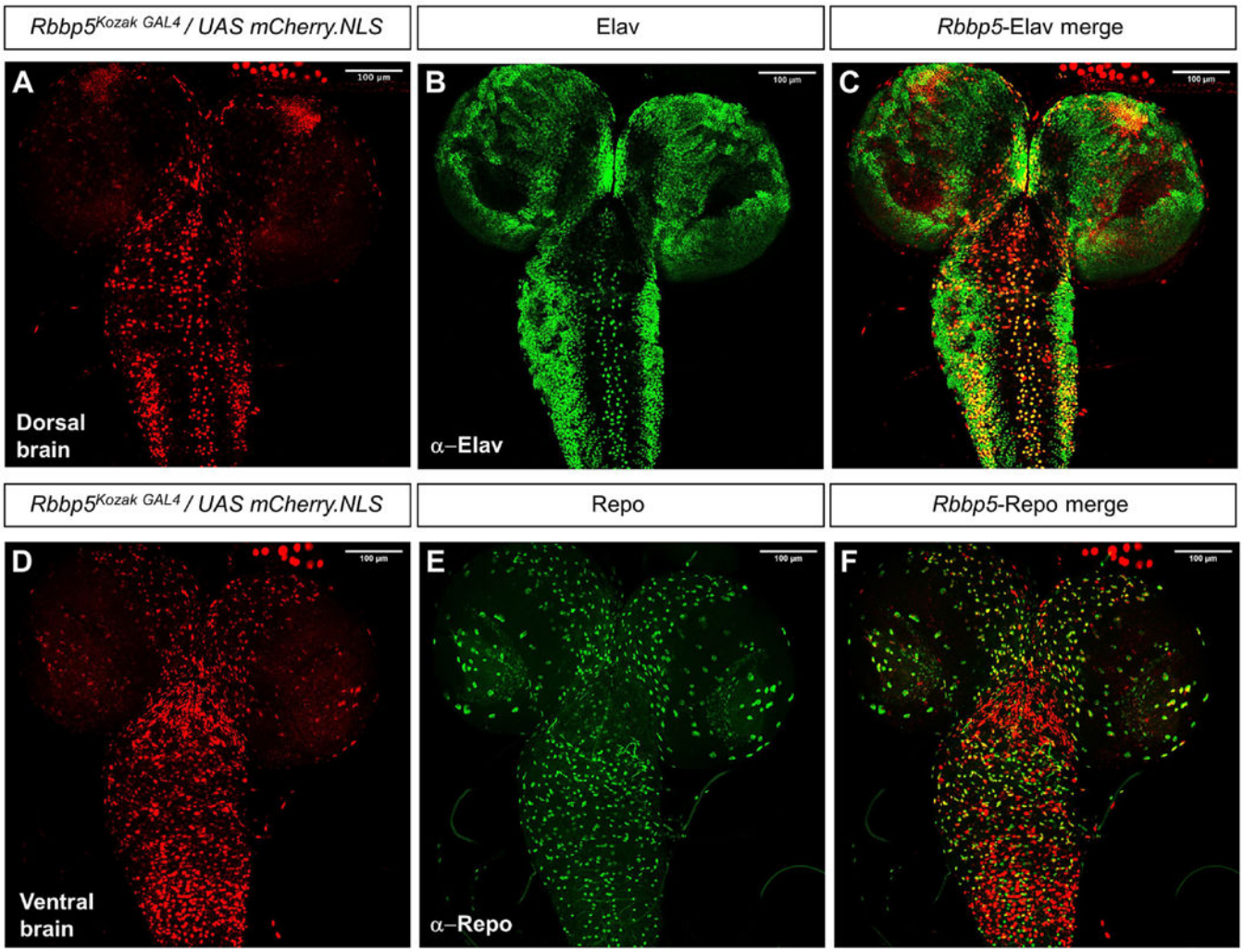

Figure 5. *Rbbp5* is expressed in a subset of neurons and glia in the *Drosophila* brain.

Rbbp5$^{Kozak\ GAL4}$*/UAS mCherry.NLS* expression pattern in the dorsal larval brain shown in (A). Elav expression in (B), and merge in (C) with co-localization in the ventral nerve cord and optic lobes of the central brain. *Rbbp5*$^{Kozak\ GAL4}$*/UAS mCherry.NLS* expression pattern in the ventral larval brain shown in (D). Repo expression in (E), and merge in (F) with co-localization in the ventral nerve cord and optic lobes.

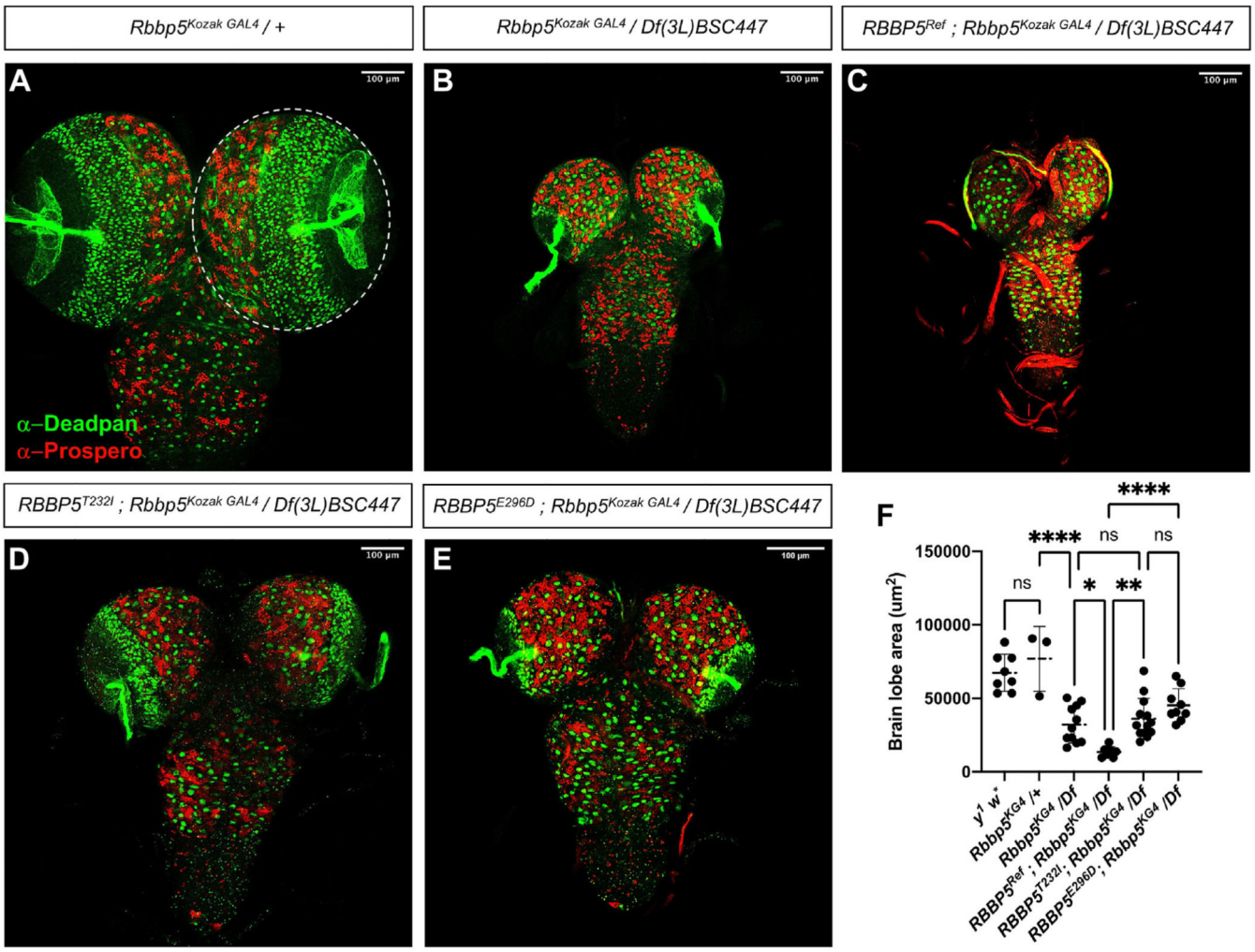

Figure 6. *RBBP5* human transgenes fail to rescue loss of *Drosophila Rbbp5*.

Heterozygous L3 *Rbbp5* loss-of-function controls (*Rbbp5*$^{Kozak\ GAL4}$/+) with Deadpan-positive neuroblasts and intermediate progenitor cells in green and Prospero-positive neural progenitor cells in red in (A). Homozygous loss-of-function with *Rbbp5*$^{Kozak\ GAL4}$ crossed to a deficiency line *Df(3L)BSC447* that includes the *Rbbp5* locus (*Rbbp5*$^{Kozak\ GAL4}$ */Df(3L)BSC447*) in (B). Attempted rescue with the human *RBBP5*^{Ref} (*RBBP5*^{Ref}; *Rbbp5*$^{Kozak\ GAL4}$*/Df(3L)BSC447*) in (C), *RBBP5*^{T232I} (*RBBP5*^{T232I}; *Rbbp5*$^{Koza\ kGAL4}$*/ Df(3L)BSC447*) in (D), *RBBP5*^{E296D} (*RBBP5*^{E296D}; *Rbbp5*$^{Kozak\ GAL4}$*/Df(3L)BSC447*) in (E). Quantification of the microcephaly phenotype (brain area) by genotype (one-way ANOVA, ns $P > .05$, *$P < .05$, **$P < .01$, ***$P < .001$, ****$P < .0001$) in (F). *RBBP5*^{Ref}, *RBBP5*^{T232I}, and *RBBP5*^{E296D} fail to rescue loss of the *Drosophila Rbbp5. RBBP5*^{Ref} expression induces a significantly more severe microcephaly phenotype than *Rbbp5*$^{Kozak\ GAL4}$*/Df(3L)BSC447*, and brain size of *Rbbp5*^{T232I}; *Rbbp5*^{KozakGAL4}*/Df(3L)BSC447* or *Rbbp5*^{E296D}; *Rbbp5*^{KozakGAL4}*/Df(3L)BSC447* larvae is not significantly different than *Rbbp5*^{KozakGAL4}*/Df(3L)BSC447*.

Genet Med. Author manuscript; available in PMC 2024 December 16.

Table 1

Summary of clinical features in affected individuals

	Individual 1	Individual 2	Individual 3	Individual 4	Individual 5
Age (year)	16	16	10	5	3
Sex	Male	Female	Male	Female	Male
Variant	c.695C>T p.(T232I)	c.762G>A p.(W254*)	c.888A>T p.(E296D)	c.919C>T p.(R307*)	c.729del p.(K244Nfs*6)
Inheritance	De novo	Unknown[a]	De novo	De novo	De novo
Gestational age	40 week	40 week	38 week	30 week	37 week
Abnormal prenatal findings	Small for gestational age	None	Echogenic intracardiac focus	Premature birth due to maternal complications[b]	Left club foot
Growth parameters	Height: 152 cm, −2.4 SD Weight: 38.6 kg, −2.7 SD HC: 53.5 cm, −1.0 SD	Height: 132 cm, −4.8SD Weight: 23.9 kg, −10.8 SD HC: 47.5 cm, −4.8 SD	Height: 117 cm, −3.0 SD Weight: 27 kg, −1.3 SD HC: 50 cm, −2.1 SD	Height: 107.5 cm, −0.7 SD Weight: 16 kg, −1.1 SD HC: 47 cm, −2.8 SD	Height: 66.5 cm, −2.0 SD Weight: 6.5 kg, −2.0 SD HC: 44.5 cm, −2.0 SD
Failure to thrive	Yes	Yes	No	No	Yes
Developmental delay	Yes	Yes	Yes	Yes	No
Intellectual disability	Yes, severe	Yes, severe	Yes, severe	Yes, mild	No
Dysmorphic features	Hypertelorism, high arched eyebrows, long eyelashes, synophrys, broad nasal tip, and retrognathia, right ear tag	Enophthalmia, long columella, mild retrognathia, right face fuller than left, microdontia	Plagiocephaly, dolichocephaly, midface hypoplasia, cupped ears, large and supernumerary teeth	Enophthalmia, short and upslanting palpebral fissures, high forehead, attached earlobe, anteverted nostrils, sparse eyebrows	Dolichocephaly, hypotelorism, sparse eyebrows, short nose, long philtrum, small and squared ears with convoluted helix, small mouth with thin lips, retrognathia
Auditory	Bilateral SNHL	Bilateral SNHL	No	No	No
Neurological	Hypotonia, dysautonomia, reduced sensation to pain and temperature	Seizure, dystonia	Generalized tonic-clonic seizures from 9.5 years of age	Hypotonia	Hypotonia
Cardiac	Two SVC	No	No	No	No
Gastrointestinal	Chronic vomiting and constipation, GERD	No	No	Anal stenosis	No
Urogenital	Cryptorchidism	No	Hypospadias	No	No
Immunological	Recurrent infection, low IgG	No	No	No	No
Musculoskeletal	Clinodactyly, prominent fingertip pad, nail hypoplasia, hyperextensible joints, delayed bone age	2nd and 3rd toe syndactyly, left pes planus	Clinodactyly brachydactyly, short 4th toe bilateral, sandal gap, pes planus, forefoot adduction	Clinodactyly	Clinodactyly, nail hypoplasia, left club foot, and hip dysplasia
Skin	Cutis marmorata	No	No	No	No
Behavior or mental	Autism, ADHD	No	Autism	N/A	No

	Individual 1	Individual 2	Individual 3	Individual 4	Individual 5
Other clinical features	Lacrimal duct stenosis, gluteal cleft	Retinal dystrophy, low visual acuity, night blindness		Prematurity, necrotizing enterocolitis	Gluteal cleft

ADHD, attention-deficit/hyperactivity disorder; *GERD*, gastroesophageal reflux disease; *HC*, head circumference; *SNHL*, sensorineural hearing loss; *SVC*, superior vena cava.

[a]The variant was not maternally inherited in the duo exome sequencing. Paternal sample was not available.

[b]Maternal complications included pulmonary arterial hypertension, preeclampsia, and gestational diabetes mellitus.